Journal of Medicinal Chemistry

PURDUE UNIVERSITY

Subscriber access provided by Purdue University Libraries

Article

Discovery of N-(4-(2,4-difluorophenoxy)-3-(6-methyl-7-oxo-6,7-dihydro-1H-pyrrolo[2,3-c]pyridin-4-yl)phenyl)ethanesulfonamide (ABBV-075/mivebresib), a Potent and Orally Available Bromodomain and Extraterminal domain (BET) Family Bromodomain Inhibitor

Keith F. McDaniel, Le Wang, Todd Soltwedel, Steven D. Fidanze, Lisa A. Hasvold, Dachun Liu, Robert A. Mantei, John K. Pratt, George S. Sheppard, Mai H Bui, Emily J Faivre, Xiaoli Huang, Leiming Li, Xiaoyu Lin, Rongqi Wang, Scott E. Warder, Denise Wilcox, Daniel H Albert, Terrance J. Magoc, Ganesh Rajaraman, Chang H. Park, Charles W. Hutchins, Jianwei J Shen, Rohinton P. Edalji, Chaohong C. Sun, Ruth Martin, Wenqing Gao, Shekman Wong, Guowei Fang, Steven W. Elmore, Yu Shen, and Warren M Kati

J. Med. Chem., **Just Accepted Manuscript** • DOI: 10.1021/acs.jmedchem.7b00746 • Publication Date (Web): 26 Sep 2017

Just Accepted

ACS Publications

Journal of Medicinal Chemistry is published by the American Chemical Society. 1155 Sixteenth Street N.W., Washington, DC 20036

Discovery of N-(4-(2,4-difluorophenoxy)-3-(6-methyl-7-oxo-6,7-dihydro-1H-pyrrolo[2,3-c]pyridin-4-yl)phenyl)ethanesulfonamide (ABBV-075/mivebresib), a Potent and Orally Available Bromodomain and Extraterminal domain (BET) Family Bromodomain Inhibitor

Keith F. McDaniel,[a,*] Le Wang,[a] Todd Soltwedel,[b] Steven D. Fidanze,[a] Lisa A. Hasvold,[a] Dachun Liu,[a] Robert A. Mantei,[a] John K. Pratt,[a] George S. Sheppard,[a] Mai H. Bui,[a] Emily J. Faivre,[a] Xiaoli Huang,[a] Leiming Li,[a] Xiaoyu Lin,[a] Rongqi Wang,[a] Scott E. Warder,[a] Denise Wilcox,[a] Daniel H. Albert,[a] Terrance J. Magoc,[b] Ganesh Rajaraman,[b] Chang H. Park,[b] Charles W. Hutchins,[a] Jianwei J. Shen,[a] Rohinton P. Edalji,[a] Chaohong C. Sun,[a] Ruth Martin,[a] Wenqing Gao,[a] Shekman Wong,[a] Guowei Fang,[a] Steven W. Elmore,[a] Yu Shen,[a] Warren M. Kati[a]

[a]*AbbVie Inc., Oncology Discovery, 1 North Waukegan Rd., North Chicago, IL 60064, USA*

[b]*Former AbbVie employee*

ABSTRACT

The development of bromodomain and extraterminal domain (BET) bromodomain inhibitors and their examination in clinical studies, particularly in oncology settings, has garnered substantial recent interest. An effort to generate novel BET bromodomain inhibitors with excellent potency and DMPK properties was initiated based upon elaboration of a simple pyridone core. Efforts to develop a bidentate interaction with a critical asparagine residue resulted in the incorporation of a pyrrolopyridone core, which improved potency by 9- to 19-fold. Additional structure-activity relationship (SAR) efforts aimed both at increasing potency and improving pharmacokinetic properties led to the discovery of the clinical candidate **63** (ABBV-075/mivebresib), which demonstrates excellent potency in biochemical and cellular assays, advantageous exposures and half-life both in animal models and in humans, as well as in vivo efficacy in mouse models of cancer progression and inflammation.

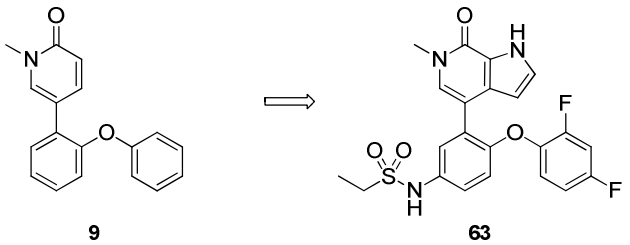

9

BRD4 TR-FRET K_i = 890 nM
BRD4 Engagement EC_{50} = 4100 nM
LipE = 1.8

63

BRD4 TR-FRET K_i = 1.5 nM
BRD4 Engagement EC_{50} = 20 nM
LipE = 4.9

▪ INTRODUCTION

The transcription of different genes is turned on or off in different cell types, explaining why, for instance, a liver cell functions differently from a nerve cell or skin cell despite all the cells within an individual having a common genetic sequence.[1] This epigenetic regulation of gene transcription is mediated, in part, by the acetylation of specific lysine residues on histone and other proteins. Proteins containing a conserved structural fold known as a bromodomain specifically bind to the acetyl-lysine marks, thereby facilitating gene transcription and other downstream events.[2] However, in some cancer and inflammatory disease states the epigenetic regulation of gene transcription is dysfunctional, resulting in the aberrant expression of growth promoting genes and pro-inflammatory cytokines.[3] Consequently, small molecules which block the acetyl-lysine/bromodomain interaction could have therapeutic utility by modulating disease specific dysfunctional gene transcription.[4]

There are 46 human proteins known to contain bromodomains and these proteins can be segregated into 8 groups based on phylogenetic/structural modeling. The Bromodomain and Extra-terminal (BET) family represents one entire group, consisting of four family members (BRD2, BRD3, BRD4 and BRDT). Each BET family member contains two N-terminal bromodomains (BDI and BDII) along with a C-terminal extraterminal domain.[5] The first BET bromodomain inhibitors to be reported, initially from the Mitsubishi Tanabe Pharmaceutical Corporation (**1a**, MS417)[6] and subsequently by the Dana Farber Cancer Institute (**1b**, JQ1),[7] incorporated the thieno[3,2-f][1,2,4]triazolo[4,3-a][1,4]diazepine core (thienotriazolodiazepine) to generate potent and selective BET bromodomain

inhibitors via occupation of the acetyl-lysine (KAc) binding site. For this core, the methyltriazole moiety mimics the acetyl-lysine group of the native peptide ligand. Additional methyltriazolodiazepines have also been developed, including clinical candidates **1c (**OTX-015)[8] and **2** (I-BET762).[9] As an alternative to the methyltriazole binding moiety, a wide variety of 3,5-dimethylisoxazoles have also been discovered, as exemplified by **3** (I-BET151).[10] Constellation Pharmaceuticals combined the 3,5-dimethylisoxazole moiety with the benzodiazepine core to generate their clinical candidate, **4** (CPI-0610).[11] Another alternative to the triazolodiazepine core utilizes the acetylated 2-methyltetrahydroquinoline core as the acetyl-lysine mimic, as exemplified by compound **5** (THQ).[12] Preclinical studies with these and other compounds have established that BET bromodomain inhibitors exhibit significant efficacy in xenograft models representing a variety of hematological and solid tumors as well as in a diverse group of inflammatory disease models. Each of these distinct BET bromodomain inhibitor cores presents novel vectors which allow access to additional binding sites of the BET bromodomain protein, with a particular focus on the incorporation of aryl groups reaching into the hydrophobic binding site known as the WPF pocket[9,13] to gain potency and selectivity. Although several compounds utilizing these cores have progressed into the clinic,[14] there remains substantial interest in the development of alternative BET bromodomain inhibitors, based upon different core structures, to provide more potent molecules along with superior pharmacokinetic properties.

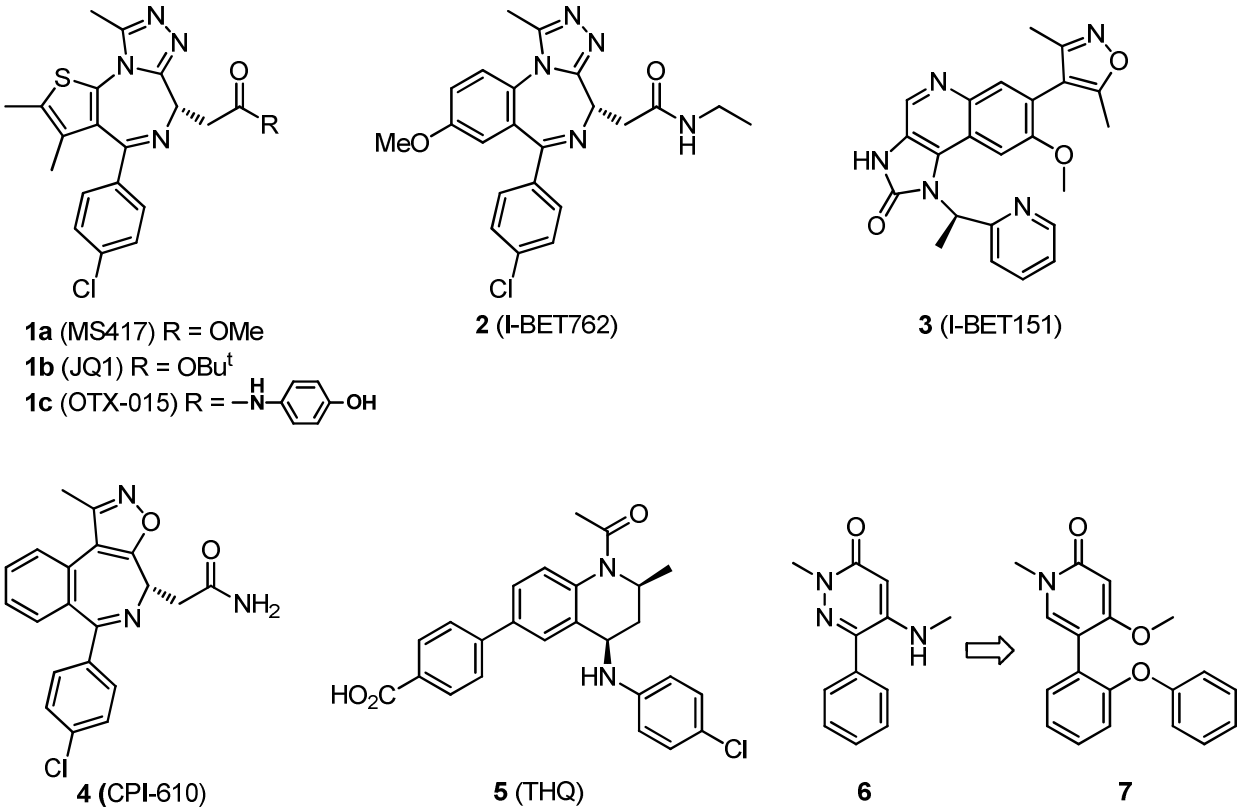

Figure 1. Representative BET bromodomain inhibitors.

We recently reported[15] the discovery of pyridazinone fragment **6** as a novel fragment core to utilize for the design of BET bromodomain inhibitors. X-ray crystallographic studies of this core demonstrated the valuable interaction of the N-methyl moiety of these pyridazinones in the amphipathic water pocket of the bromodomain protein, as well as the binding of the pyridazinone carbonyl with the NH_2 of Asn433.[15] SAR efforts led to the replacement of the pyridazinone of **6** by pyridone and incorporation of a crucial biphenyl ether moiety to generate N-methylpyridone BET bromodomain inhibitors based upon compound **7**. Utilization of this core provided inhibitors demonstrating sub-μM activity in TR-FRET binding assays against BRD4, and substantial efficacy in several in vivo mouse xenograft models.[15] Herein we describe the SAR development leading from this pyridone core to the discovery of pyrrolopyridone-based inhibitor **63** (ABBV-075/mivebresib), an extremely potent BET

bromodomain inhibitor demonstrating excellent pharmacokinetic properties which currently is undergoing Phase I clinical trials (ClinicalTrials.gov identifier: NTC02391480).[16]

▪ SYNTHESIS

Synthesis of the inhibitors described and characterized herein relied mainly upon a Suzuki-Miyaura cross coupling reaction[17] to form the bond between the pyridone-based core and the biaryl ether, as is depicted in its simplest form for the generation of pyridones **9**, **11**, and **13** in Scheme 1. Thus, reaction of 2-phenoxyphenylboronic acid with bromo pyridones **8**, **10**, or **12** under standard Suzuki-Miyaura coupling conditions provided compounds **9**, **11**, and **13** in good yield.

Scheme 1[a]

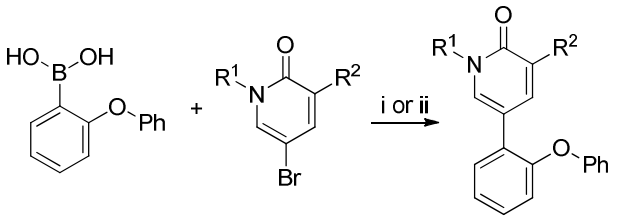

8 R^1 = Me, R^2 = H **9** R^1 = Me, R^2 = H
10 R^1 = H, R^2 = Me **11** R^1 = H, R^2 = Me
12 R^1 = Me, R^2 = NH_2 **13** R^1 = Me, R^2 = NH_2

[a] Reagents and conditions: (i) $Pd(PPh_3)_4$, CsF, DME/MeOH, 120 °C, 79% (**9**), 82% (**13**); (ii) $Pd(PPh_3)_2Cl_2$, Na_2CO_3, DME/MeOH, 120 °C, 23% (**11**).

An analogous approach provided access to the unadorned pyrrolopyridone **19**. Pyrrolopyridone bromide **18** was generated in excellent overall yield utilizing a five-step sequence beginning with 5-bromo-2-methoxy-4-methyl-3-nitropyridine (**14**), and was utilized in the crucial Suzuki-Miyauri coupling reaction with 2-phenoxyphenylboronic acid followed by deprotection to form **19** (Scheme 2).

Scheme 2[a]

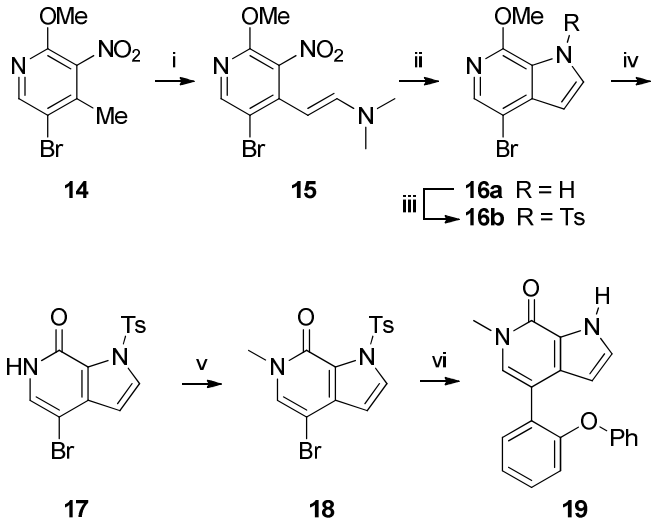

[a] Reagents and conditions: (i) LiOMe, DMF, 100 °C, 76%; (ii) Ra-Ni 2800, ethyl acetate, rt, 72%; (iii) NaH, pTsCl, DMF, rt, quant. yield; (iv) 4 M HCl, 1,4-dioxane, 40 °C, 94%; (v) NaH, MeI, DMF, rt, 96%; (vi) 2-phenoxyphenylboronoic acid, $Pd(PPh_3)_4$, CsF, DME/ MeOH, 120 °C, then add K_2CO_3, water, 120 °C, 59%.

Three complimentary approaches detailed in Schemes 3-5 were used to prepare more highly functionalized pyrrolopyridone analogs, incorporating substitution on both aryl groups of the crucial biaryl ether. Two crucial transformations, a Suzuki coupling and a nucleophilic aromatic substitution, were carried out in each approach, although the order of these two transformations was altered based upon ease of synthesis and the availability of starting materials. The first of these three approaches is outlined in Scheme 3 for the generation of compounds **24-27**, which were prepared in order to explore SAR on the central aryl ring. This approach began with a Suzuki-Miyaura coupling reaction of bromide **18**, which was reacted with aryl boronic acid **20** to form the biaryl intermediate **21**. With this biaryl core in place, generation of biaryl ether **22** was accomplished readily via an S_NAr displacement reaction of the activated aryl fluoride of **21** by phenol in the presence of cesium carbonate. The tosyl protecting group was also removed during this transformation. Iron-catalyzed reduction of the nitro group of **22** in

the presence of ammonium chloride followed by functionalization of the resulting aniline **23** provided facile access to sulfonamides **24-26** and sulfamide **27**.

Scheme 3[a]

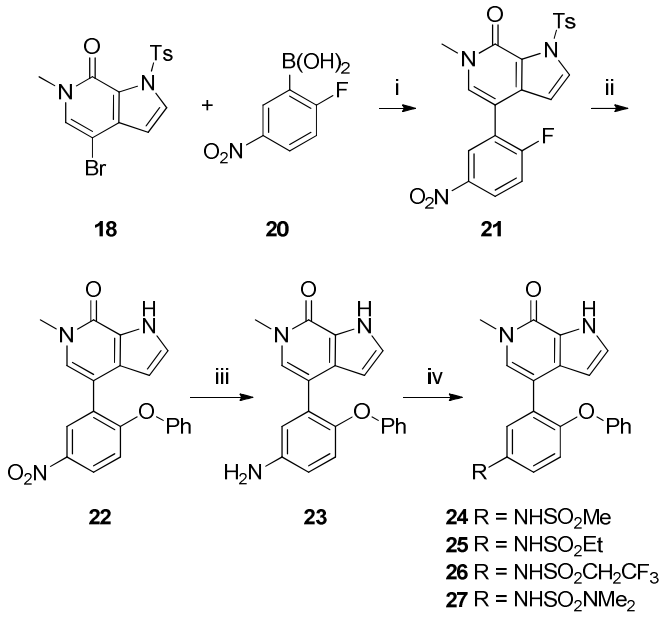

[a]Reagents and conditions: (i) $Pd(PPh_3)_4$, Na_2CO_3, DME/water, 120 °C, 52%; (ii) Phenol, Cs_2CO_3, DMSO, 100 °C, 72-84%; (iii) Fe, NH_4Cl, THF/EtOH/H_2O, 95 °C 82% (**23**); (iv) RSO_2Cl, NEt_3, CH_2Cl_2, rt, then 1N NaOH, 90 °C, 45-77% (**24-26**) or Me_2NSO_2Cl, Cs_2CO_3, DMF, 80 °C, 11% (**27**).

The second general approach to the formation of inhibitors containing functionalized biaryl ethers is outlined in Scheme 4. The central premise of this approach relied upon formation of the functionalized biaryl ether as the first step in the sequence, followed by Suzuki-Miyaura coupling with pyrrolopyridone boronate **28** to generate the complete inhibitor framework. To facilitate this approach, pyrrolopyridone boronate **28** was generated in good yield by reaction of bromide **18** with 4,4,4',4',5,5,5',5'-octamethyl-2,2'-bi(1,3,2-dioxaborolane) in the presence of tris(dibenzylideneacetone)dipalladium(0), X-PHOS, and potassium acetate. The availability of boronate

28 allowed for the use of aryl bromides and iodides as biaryl ether coupling partners, which simplified the incorporation of a wide variety of more highly functionalized analogs into the SAR evaluation and also provided a more convergent synthetic approach. For example, S_NAr reaction of 3-bromo-2-chloro-5-nitropyridine (**29**) with phenol provided brominated biaryl ether **30** in excellent yield (Scheme 4). Coupling of pyrrolopyridone boronate **28** with biaryl ether bromide **30** produced protected pyrrolopyridone **31** in excellent yield. Reduction of the nitro group of **31** followed by sulfonylation and removal of the tosyl protecting group of **32** gave pyridine sulfonamide **33** in excellent overall yield.

Scheme 4[a]

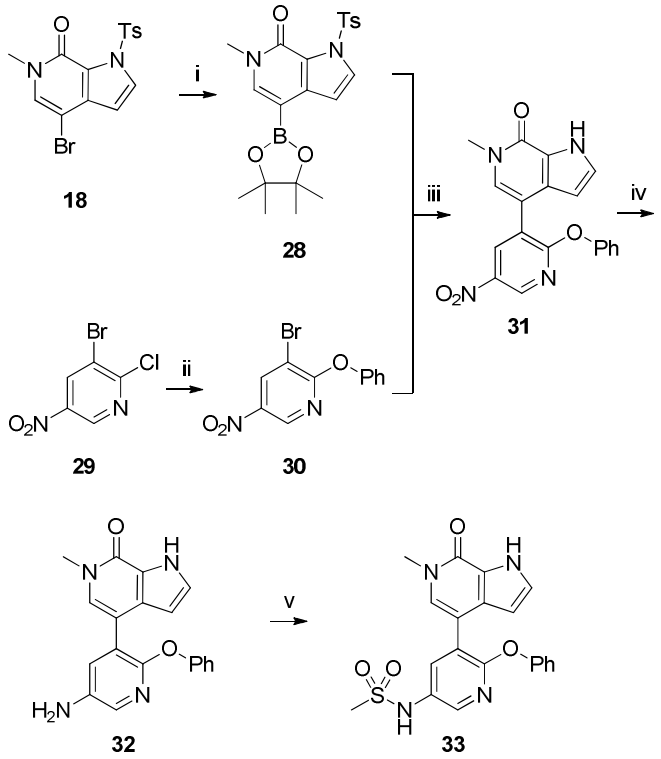

[a]Reagents and conditions: (i) 4,4,4',4',5,5,5',5'-octamethyl-2,2'-bi(1,3,2-dioxaborolane, KOAc, $Pd_2(dba)_3$, X-PHOS, 1,4-dioxane, 80 °C, 73%; (ii) Phenol, Cs_2CO_3, DMSO, 80 °C, 91%; (iii) KOAc, $Pd_2(dba)_3$, (1,3,5,7-tetramethyl-6-phenyl-2,4,8-trioxa-6-phosphaadamantane), 1,4-dioxane/H_2O, 60 °C, quant. yield; (iv) Fe, NH_4Cl, THF/EtOH/H_2O, 100 °C, quant. yield; (v) $MeSO_2Cl$, NEt_3, CH_2Cl_2, rt, then 1 M NaOH, 90 °C, 77%.

The third approach to the generation of pyrrolopyridone inhibitors employed an even more convergent synthetic sequence (Scheme 5), and utilizes the crucial Suzuki-Miyaura coupling as the final step in the sequence. For example, S_NAr displacement of **34** by phenol, subsequent reduction of the nitro group of **35,** and functionalization of the resulting aniline **36** provided fully functionalized sulfonamide **37**, suitable for coupling with boronate **28** to establish an alternate route to inhibitor **24**. As exemplified by the routes highlighted in Schemes 3-5, the availability of multiple potential approaches to each compound ensured that synthetic availability was not a limiting factor for the SAR evaluation of these inhibitors. All of the additional inhibitors examined in this study were generated by the straight-forward application of one of the approaches outlined in Schemes 3, 4, or 5, including compound **63** from compound **21** via the approach outlined in Scheme 3 as described in the Experimental Section. Detailed experimental procedures and characterization of compounds **38-62** and **64-120** can be found in the Supporting Information (Schemes S1-7).

Scheme 5[a]

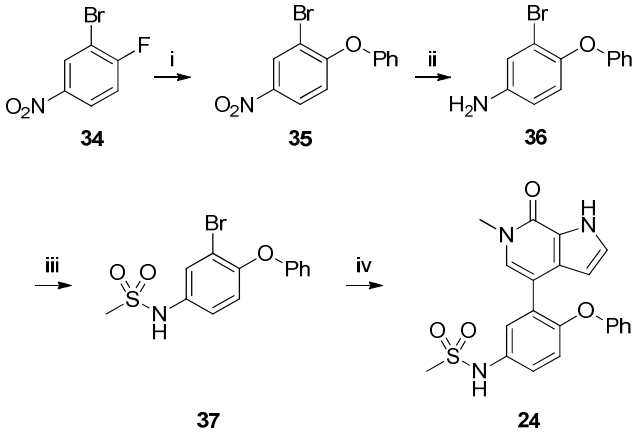

[a]Reagents and conditions: (i) Phenol, Cs_2CO_3, DMSO, 80 °C, quant. yield; (ii) Fe, NH_4Cl, THF/EtOH/H_2O, 100 °C, quant. yield; (iii) NEt_3, $MeSO_2Cl$, CH_2Cl_2, rt, then NaOH, 1,4-dioxane, 70 °C, 75% (iv) **28**, KOAc, $Pd_2(dba)_3$, (1,3,5,7-tetramethyl-6-phenyl-2,4,8-trioxa-6-phosphaadamantane), 1,4-dioxane/H_2O, 60 °C, 79%.

▪ RESULTS AND DISCUSSION

To further improve the potency of pyridone-based BET bromodomain inhibitors such as **7**, exploration of compounds that might provide an even more productive interaction between the inhibitor core and the conserved Asn433 residue of the BET protein was undertaken. Compounds were evaluated using a time-resolved fluorescence resonance energy transfer (TR-FRET) binding assay and two complementary cellular assays. The TR-FRET binding assay was used to determine the affinities (K_i) of compounds for a construct containing the two bromodomains of BRD4. Target engagement in cells was measured using a luciferase reporter assay based on the contribution of BRD4 to human papilloma virus (HPC) E2-mediated transcriptional repression, where BRD4 is part of the HPV long control region (LCR) promoter repression complex with E2 and EP400.[18] In this assay, engagement of BRD4 with a BET bromodomain inhibitor de-represses the HPV promoter engineered to drive luciferase transcription, resulting in an increase of luciferase signal (see Supporting Information, Figure S3). Cancer cell lines are dependent on BET proteins for growth,[19] and so, as an orthogonal cellular assay, the impact of compounds on cancer cell proliferation was measured using the triple negative breast cancer cell line MX-1 (ATCC) in a 3-day proliferation assay. Good correlation was observed between the two cellular assays, an indication that cell killing is the result of engagement of the BRD4 target (Supporting Information, Figure S5). Examination of the protein-inhibitor co-crystal X-ray structures of pyridazinone **6** and related pyridone analogs indicated that although the carbonyl moieties of these cores are situated at an ideal distance away from the Asn433 NH_2 group (2.9 Å for **6**),[15] there does not appear to be a productive contact between the Asn433 amide carbonyl and the pyridazinone or pyridone. The first structural motif to be examined in order to provide a bidentate interaction with Asn433 incorporated the 3-methyl NH-pyridone **11** in place of the N-methyl pyridone core of **9**. It was proposed that a bidentate interaction between the NH of the pyridone and the Asn433 carbonyl would provide an improved binding interaction while maintaining the previous positive interactions of both the methyl

group with the amphipathic water pocket and the carbonyl group of the pyridone with the Asn433 amide NH_2 moiety. Examination of NH-pyridone **11** revealed, however, no improvement in biochemical or cellular activity compared to N-methyl pyridone **9** (Table 1), and in fact revealed a slight decline in LipE.[20] An X-ray structure of pyridone **11** bound in BRD4 BDII (PDB code: SUVZ) indicated that while the pyridone

Table 1. Biochemical and cellular potency of compounds 9, 11, 13, and 19.

	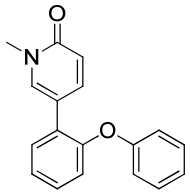	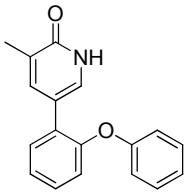	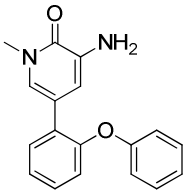	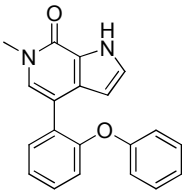
Compound ID	**9**	**11**	**13**	**19**
BRD4 TR-FRET K_i (μM)[a]	0.89 ± 0.037	1.7 ± 0.06	3.0 ± 0.86	0.048 ± 0.001
MX-1 Proliferation EC_{50} (μM)[b]	4.8	2.4	> 5	0.55
BRD4 Engagement EC_{50} (μM)[b]	4.1	2.3	8.5	0.48
LipE	1.8	1.5	2.0	2.8

[a]TR-FRET BRD4 K_i values are reported as the geometric mean derived from 3 or more independent measurements. [b]EC_{50} values are reported as the mean derived from two measurements.

carbonyl/Asn433-NH_2 distance remained optimal (2.9 Å), there is not a direct interaction of the pyridone NH with the Asn433 carbonyl moiety but instead a water-mediated association (Figure 2) which does not provide additional binding compared to pyridone **9**. The slightly weaker K_i of NH-pyridone **11** compared to N-methylpyridone **9** may be a reflection of the presence of a fixed water molecule between the NH of **9** and the Asn433 carbonyl.[21] The entropy cost of rigidifying the water may affect the K_i

negatively. SZMAP calculation[21] of the ΔG of this water gives a value of -6.64 kcal/mol. While one cannot compare this free-energy value directly with energy values derived from binding data, the low value indicates the water may have high occupancy.

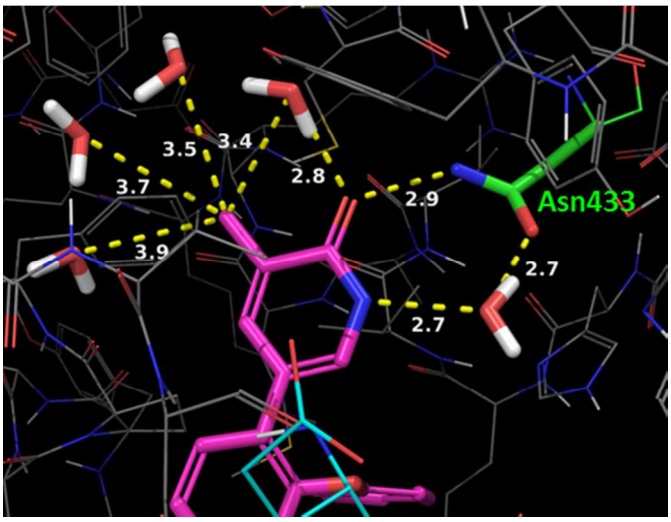

Figure 2. Compound **11** bound to BRD4 BDII (Resolution = 1.6 Å, PDB code: SUVZ). Leu387 and Gly386 removed for clarity.

In a second attempt to generate a more productive bidentate interaction between the crucial Asn433 moiety and the pyridone inhibitor, it was next hypothesized that incorporation of an amine NH group one atom closer to the Asn433 carbonyl would position the requisite NH group in a more suitable location. Binding of this core would also be likely to displace a water molecule in the structure of pyridone **11**. Thus, 3-amino-1-methylpyridone **13** was generated and examined (Table 1). Binding and cellular data for **13**, however, indicated that this exocyclic amine moiety also failed to provide any improvement in potency. A slight improvement in LipE was realized, mainly a result of a lower cLogP. A substantial improvement in biochemical binding potency, cellular activity, and lipophilic efficiency was realized, however, with the incorporation of a pyrrole, in the form of pyrrolopyridone **19** (Table 1). Compared to pyridone **9**, addition of the pyrrole of **19** improved both biochemical and cellular activity by 9- to 19-fold (Table 1).[22] Examination of the X-ray co-crystal structure of pyrrolopyridone **19** (PDB

code: SUVY) in BRD4 BDII revealed the basis for this boost in activity (Figure 3). In addition to maintaining the valuable interactions of the phenyl ether moiety in the WPF pocket, the N-methyl group in the amphipathic water pocket, and the pyridone carbonyl with the NH_2 of Asn433, the X-ray structure confirms that a valuable interaction between the pyrrole NH and the Asn433 carbonyl has been introduced, with an ideal 2.8 Å distance measured between these two moieties. In addition, the pyrrole ring of the heterocycle displaces a water molecule which is in a hydrophobic environment; the free-energy of this water is +1.2 kcal/mol.[21] The combination of replacing the water molecule bound to the Asn433 carbonyl with a good hydrogen bond donor and replacing a water molecule in a hydrophobic environment with the hydrophobic pyrrole ring would be expected to improve affinity, as demonstrated by an improvement in K_i from 890 nM to 48 nM.

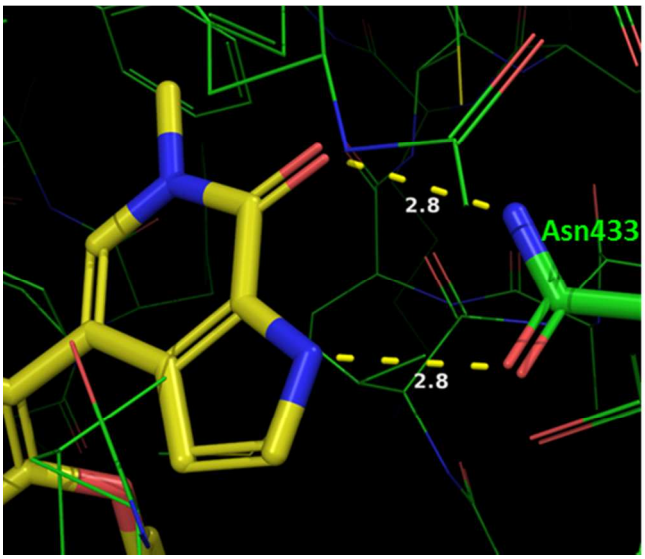

Figure 3. Compound **19** (yellow) bound to BRD4 BDII (Resolution = 2.3 Å, PDB code: SUVY). Tyr432 removed for clarity.

With an effective and potent pyrrolopyridone BET bromodomain inhibitor core in place, examination of SAR at additional sites on the molecule was undertaken to further improve potency and to assess DMPK properties. The first region of the protein to be investigated was the area accessible

from the central aryl ring of the core, reaching into the pocket bounded by the ZA loop[23] of the protein and the adjacent helix. In fact, access to this pocket was facilitated by the chemistry developed to generate biaryl ethers, as described above. In general, incorporation of an electron-withdrawing group, such as a nitro group, an ester, or a sulfone, promoted nucleophilic aromatic substitution on this central ring, and allowed for rapid synthesis of the biaryl ether moiety with a functional group attached para to the ether oxygen. Examination of the SAR available directly from this functional group on the central ring, or after additional manipulation of this functional group, revealed a wide range of substituents with the potential for substantial positive protein backbone interactions (Table 2). For example, nucleophilic substitution on the central aryl moiety containing a nitro group, followed by reduction of the nitro group and formation of sulfonamides provided compounds **24**-**26**, which all demonstrated improved potency in the TR-FRET binding assay and in cellular assays compared to the unsubstituted analog **19**, along with a considerable improvement in lipophilic efficiency (e.g., LipE for **19** = 2.8, LipE for **24** = 5.3). An X-ray co-crystal structure of sulfonamide **24** (PDB code: SUVX) in BRD4 BDII (Figure 4) confirmed the presence of a productive hydrogen bond between the NH of Asp381 and one of the sulfonamide oxygens, with a measured distance of 2.8 Å. Notably, the positioning of the sulfonamide moiety allowed for the formation of this hydrogen bond without disturbing the valuable interactions between the pyrrolopyridone carbonyl (2.9 Å) and the pyrrole NH (2.9Å) with Asn433 and also maintained the critical position of the phenyl ether in the WPF pocket. A similar interaction and boost in potency was noted with the analogous pyridone BET bromodomain inhibitor core[15] and also with a related 2-methylpyrrole-3-carboxaminde core.[24] Similar increases in potency were demonstrated for sulfamides (**27**) and amides (**39**), although not to the extent shown for sulfonamides. Analogs were also prepared that incorporated a hydrogen bond accepting group directly attached to the central aryl group, including reversed amides (**45** and **46**), sulfones (**51**), and reversed sulfonamides (**56**). Although these analogs also demonstrated improved potency compared to the unsubstituted analog **19**, this increased potency was not as substantial as for sulfonamides **24**-**26**. We hypothesize that for these moieties to be

positioned in the proper alignment and distance to take advantage of an interaction with Asp381, torqueing of the biaryl bond between the central aryl group and the pyrrolopyridone is necessary, thus requiring a repositioning of the phenyl ether into a less favorable arrangement in the WPF pocket.

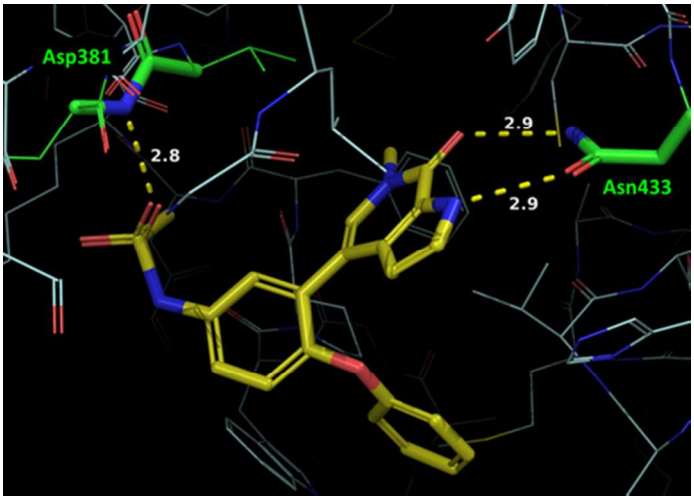

Figure 4. Compound **24** (yellow) bound to BRD4 BDII (Resolution = 1.5Å, PDB code: SUVX). Leu385 removed for clarity.

In addition to the enhanced potency achieved by incorporation of hydrogen bond acceptors on the central aryl group, a substantial improvement in the *in vitro* stability of these compounds in liver microsomes was also evident compared to unsubstituted analog **19**. For example, whereas the stability of compound **19** was limited in human liver microsomes and particularly poor in mouse and rat liver microsomes, sulfonamides **24-26** and **33** demonstrated excellent stability in human liver microsomes and moderate stability in mouse microsomes (Table 2). The MDCK cell permeability of these compounds was high (> 10 x 10^{-6} cm/s), although compounds containing a central pyridine ring (e.g., **33**) demonstrated only moderate permeability.

Table 2. Activity and ADME data for aryl substitutions.

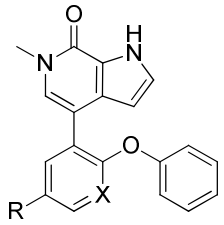

			TR-FRET BRD4	MX-1 Proliferation	BRD4 Engagement	Liver Microsome $Cl_{int,u}$[c]			MDCK Permeability[d]
ID	X	R	K_i (nM)[a]	EC_{50} (nM)[b]	EC_{50} (nM)[b]	Human	Mouse	Rat	10^{-6} cm/s
						L/hr/kg			
19	CH	H	48 ± 1.4	550	480	100	5600	2400	31
24	CH	-$NHSO_2Me$	2.4 ± 1.1	16	11	5.0	18	120	12
25	CH	-$NHSO_2Et$	1.5 ± 0.2	14	8.1	< 2.7	55	200	22
26	CH	-$NHSO_2CH_2CF_3$	4.4 ± 0.4	31	22	2.8	39	76	16
27	CH	-$NHSO_2NMe_2$	2.9 ± 0.1	65	43	14	140	240	19
33	N	-$NHSO_2Me$	4.1 ± 0.3	46	88	3.8	< 5.6	36	6
39	CH	-NHCOMe	9.8 ± 1.5	46	26	6.8	210	46	28
45	CH	-$CONH_2$	14 ± 1.4	120	71	2.9	27	33	14
46	CH	-CONHEt	32 ± 3.9	130	70	4.1	43	240	30
51	CH	-SO_2Me	5.8 ± 0.2	52	50	5.5	23	65	24
56	CH	-SO_2NH_2	3.6 ± 0.1	56	39	< 2.6	31	79	22

[a]TR-FRET BRD4 K_i values are reported as the geometric mean derived from 3 or more independent measurements; [b]EC_{50} values are reported as the mean derived from two measurements; [c]For reference, average in-house positive control clearance values for dextromethorphan and verapamil, respectively, are $Cl_{int,u}$ (human) = 7.4 L/hr/kg (low) and $Cl_{int,u}$ (human) = 30 L/hr/kg (high). [d]For reference, average in-house positive control permeability values for atenolol and metoprolol, respectively, are 0.5 x 10^{-6} cm/s (low) and 36 x 10^{-6} cm/s (high).

With analogs in hand that demonstrated excellent potency and promising in vitro microsomal stability and permeability properties, the pharmacokinetic properties of lead compounds were examined.

The general trend observed for these compounds is exemplified by the mouse and rat PK data collected for sulfonamide **24**. In agreement with the mouse liver microsome stability data ($Cl_{int,u}$ = 18 L/hr/kg), sulfonamide **24** exhibited moderately low unbound IV clearance (39 L/hr/kg) and good oral absorption (FaFg = 0.77) leading to reasonable oral exposures (AUC = 0.34 μM*hr, F = 55%) in mouse PK studies. However, rat PK studies for **24** exhibited substantially higher clearance (IV $Cl_{p,u}$ = 74 L/hr/kg), with limited oral absorption (FaFg = 0.32) and exposure (AUC = 0.016 μM*hr) leading to poor bioavailability (F = 10%). A metabolic pathways analysis of **24** in rat and human liver microsomes (Figure S2 and Table S1, Supporting Information) revealed that extensive oxidative metabolism in rat liver microsomes occurs at the unsubstituted phenyl ether moiety, as might be expected for this electron-rich substrate. This study also indicated that cleavage of the phenyl ether and N-demethylation at the N-methyl substituent on the pyrrolopyridone provide additional metabolites, but these metabolic liabilities were much less significant compared to oxidation of the phenyl ether. Oxidation of the unsubstituted phenyl ether of **24** was also determined to be the main metabolic pathway in human liver microsomes, although this metabolism was less extensive in human liver microsomes than in rat liver microsomes.

To overcome the metabolic liabilities posed by the unsubstituted phenyl ether of analogs such as **24** and **25**, a set of analogs was generated to examine the scope and limitations of replacements for this phenyl ether, examining these analogs on core structures that contained either a methyl or ethyl sulfonamide on the central phenyl ring (Table 3). It was hoped that the incorporation of electron-withdrawing substituents on the phenyl ether ortho or para to the ether oxygen would substantially reduce the metabolic instability of this moiety, and thus most of the initial analogs generated contained halogenated phenyl ethers or other electron-poor substituents (Table 3, compounds **57**-**64**). Initial results from this evaluation indicated that the incorporation of more electron-poor phenyl ethers did in general provide compounds with substantially improved stability in rat liver microsomes, a trend also noted for similarly substituted N-methylpyridone[15] and 2-methylpyrrole-3-carboxamide[24] BET bromodomain inhibitors. Incorporation of one halogen (**57**) or multiple halogens (**61**-**64**) gave

compounds with 6- to 34-fold improvement in rat liver microsome stability, while generally maintaining potency in both the biochemical binding assay and in cellular assays. Phenyl ethers substituted with nitriles (**58**) or trifluoromethyl groups (**59**, **60**) also provided improved stability in rat liver microsomes, although in the case of the trifluoromethyl substituents this improvement came at the expense of stability in mouse liver microsomes and also overall potency. Examination of heteroaryl replacements (**65**, **66**) failed to provide inhibitors that improved liver microsome stability while maintaining potency. Of these aryl analogs, 2,4-difluorophenyl ethers **62** and **63** provided the best combination of potency and stability.

In addition to aryl replacements for the unsubstituted phenyl ethers of **24** or **25**, compounds containing alkyl replacements were also examined. Benzyl ether **67**, which incorporates a methylene spacer in the ether moiety, lost substantial potency compared to the phenyl ethers. Cyclohexyl ether **68** maintained the potency of the phenyl ethers, but failed to provide an improvement in metabolic stability. Attempts to improve the ADME properties of this cyclohexyl moiety by replacement with tetrahydropyran (**69**) or with the 4,4-difluorinated cyclohexyl analog **70** also gave compounds with reduced potency or limited metabolic stability, and also inadequate permeability. Acyclic analogs such as **71** lost substantial potency compared to aryl ethers. Incorporation of hydrophilic moieties, represented by dimethylamine **72** or piperidine **73**, led to improved liver microsome stability, but both the potency and permeability of these compounds was limited. Since none of these alkyl analogs provided potency or ADME properties comparable to 2,4-difluorophenylether analogs **62** and **63**, all additional efforts focused on the examination of compounds containing this moiety.

Table 3. Activity and ADME data for phenyl ether replacements

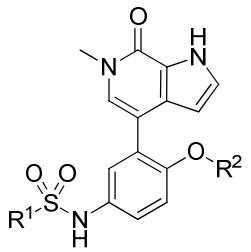

			BRD4	MX-1	BRD4	Liver Microsome $Cl_{int.u}$[c]			MDCK
			TR-FRET	Proliferation	Engagement	Human	Mouse	Rat	Permeability[d]
ID	R^1	R^2	K_i (nM)[a]	EC_{50} (nM)[b]	EC_{50} (nM)[b]		L/hr/kg		10^{-6} cm/s
24	Me	Ph	2.4 ± 1.1	16	11	5.0	18	120	12
25	Et	Ph	1.5 ± 0.2	14	8.1	< 2.7	55	200	22
57	Et	*p*-Cl-phenyl	3.4 ± 0.3	22	17	< 5.8	54	12	21
58	Et	*p*-CN-phenyl	9.4 ± 2.5	17	48	2.5	< 6.5	4.9	11
59	Et	*p*-CF_3-phenyl	9.0 ± 0.4	30	65	7.7	170	35	11
60	Me	*o*-CF_3-phenyl	6.4 ± 0.9	83	76	32	81	15	7.8
61	Me	2-Cl-4-F-phenyl	3.1 ± 0.7	27	35	14	51	19	11
62	Me	2,4-di-F-phenyl	4.5 ± 0.6	29	21	9.3	17	< 3.9	17
63	Et	2,4-di-F-phenyl	1.5 ± 0.2	13	20	< 2.9	33	< 4.9	29
64	Et	2,4,6-tri-F-phenyl	12 ± 4.8	7.9	19	6.1	54	14	21
65	Me	3-pyridyl	6.3 ± 2.8	34	67	5.2	32	21	3.0
66	Et	5-pyrimidine	32 ± 1.5	130	170	< 2	14	2.9	1.0
67	Me	benzyl	68 ± 1.7	110	120	7.3	54	34	24
68	Me	cyclohexyl	3.7 ± 0.3	14	18	27	220	96	23
69	Me	4-tetrahydro-pyran	68 ± 15	72	90	< 1.8	< 5.4	14	1.7
70	Me	4,4-di-F-cyclohexane	19 ± 1.0	19	20	< 2.3	43	12	12

71	Et	-CH_2CMe_3	38 ± 20	77	79	17	62	26	43
72	Et	4-(dimethyl-amino)cyclohexyl	26 ± 2.8	86	270	< 1.6	7.5	< 2.7	2.7
73	Et	1-methyl-piperidin-4-yl	430 ± 45	210	880	< 1.7	< 5.1	4.8	0.55

[a]TR-FRET BRD4 K_i values are reported as the geometric mean derived from 3 or more independent measurements; [b]EC_{50} values are reported as the mean derived from two measurements; [c]For reference, average in-house positive control clearance values for dextromethorphan and verapamil, respectively, are $Cl_{int,u}$ (human) = 7.4 L/hr/kg (low) and $Cl_{int,u}$ (human) = 30 L/hr/kg (high). [d]For reference, average in-house positive control permeability values for atenolol and metoprolol, respectively, are 0.5 x 10^{-6} cm/s (low) and 36 x 10^{-6} cm/s (high).

PK studies were next undertaken to assess whether or not the improvements in rat liver microsome stability for 2,4-difluorophenyl ethers **62** and **63** compared to unsubstituted phenyl ether **24** would translate into improved rat PK properties. Examination of the rat PK of **62** and **63** revealed a substantial improvement in IV clearance and absorption (FaFg), leading to higher bioavailability and improved oral exposures (Table 4). In addition, modest improvement in mouse PK in both clearance and bioavailability for 2-4-difluorophenyl analogs **62** and **63** was noted compared to phenyl analog **24**. Furthermore, ethyl sulfonamide **63** was preferred over methyl sulfonamide **62** based upon its modestly improved biochemical and cellular activity together with its low clearance in human liver microsomes. Compound **63** also exhibited physiochemical properties typically targeted for the generation of drug-like molecules,[20,25] including molecular weight (459 g/mol), cLogP (3.8), TPSA (92 Å), number of H-bond acceptors (4) and donors (2), and LipE (4.9).

Table 4. DMPK data for compounds 24, 62 and 63.

	Mouse PK (3 mg/kg iv and 10 mg/kg po)				Protein Binding Mouse	Rat PK (1 mg/kg iv and po)				Protein Binding Rat
ID	IV $Cl_{p,u}$[a]	PO AUC_u[b]	FaFg[c]	F (%)	($f_{u,plasma}$)[d]	IV $Cl_{p,u}$[a]	PO AUC_u[b]	FaFg[c]	F (%)	($f_{u,plasma}$)[d]
24	39	0.34	0.77	55	0.039	74	0.016	0.32	10	0.034
62	10	1.3	0.70	65	0.033	25	0.19	0.52	40	0.036
63	19	0.63	0.90	83	0.020	27	0.27	0.77	65	0.023

[a]$Cl_{int,u}$ [L/hr/kg]; [b]AUCu [μM*hr]; [c]FaFg = F/(1-Clp/Qh). Qh = liver blood flow for mouse: 5.2 L/hr/kg; for rat: 3.8 L/hr/kg;

[d]$f_{u,plasma}$ (unbound fraction in plasma)

Although difluorophenyl ether sulfonamide **63** displayed the desired potency and DMPK properties to support moving this compound forward toward clinical candidate consideration, a final round of SAR was carried out holding the 2,4-difluorophenyl ether moiety in place and re-examining a wider range of substituents on the central aromatic ring. This effort is described in the Supporting Information (Table S3). It was found that incorporation of certain substituents on this central aromatic ring also provided potent and stable compounds. However, compound **63** demonstrated a superior combination of attributes including excellent potency in cellular assays and an advantageous pharmacokinetic profile. Compound **63** also compared favorably in terms of biochemical binding potency and cellular activity with known BET inhibitors such as **1b**[7]and **1c**[8] (see Table S1 in the Supporting Information). Thus, ethyl sulfonamide **63** was chosen as the lead compound and was examined in a variety of in vitro and in vivo efficacy experiments.

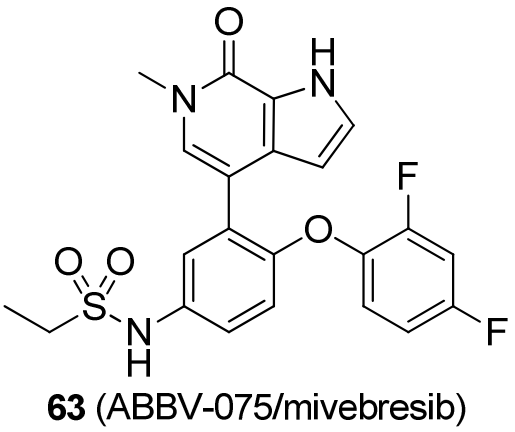

63 (ABBV-075/mivebresib)

Figure 5. Structure of compound **63**

Compound **63** displayed cellular activities characteristic of BET family inhibitors, such as inhibition of c-Myc expression and displacing BRD4 from the Myc promoter.[26] On-target inhibition with compound **63** was also confirmed in vivo by assessing the effect on cytokine release in a murine model of LPS-induced endotoxic shock. The acute upregulation of inflammatory cytokine genes such as IL-6 observed in the shock model has been shown to be BET-mediated and consequently cytokine inhibitory responses can be considered as a biomarker of BET bromodomain inhibition.[9,27] As shown in Figure 6a, oral administration of compound **63** resulted in a dose-dependent inhibition of IL-6 concentration measured in plasma two hours post LPS challenge. The magnitude of inhibition correlated with the concentration of compound **63** in plasma at the time of cytokine measurement (Figure 6b). These results indicate that robust target inhibition (>50%) was achieved with plasma concentrations ranging from 0.03 to 0.1 μM.

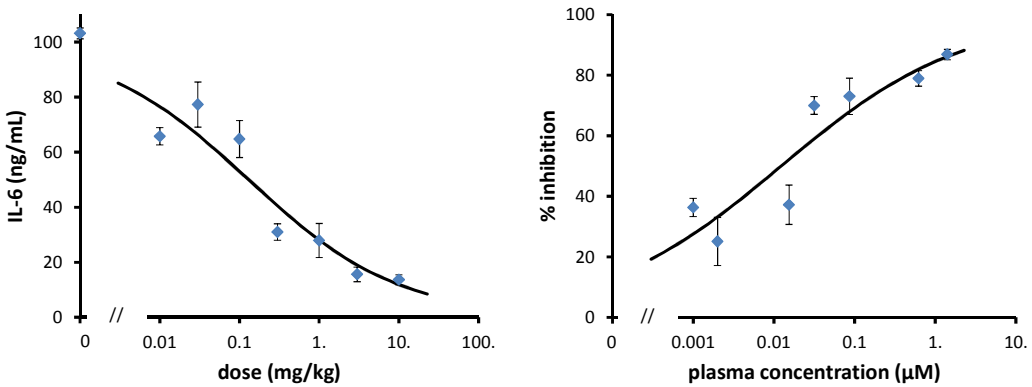

(a) **(b)**

Figure 6. (a) Dose–dependent inhibition of LPS-induced IL-6 by compound **63**. (b) Relationship between plasma concentration of compound **63** and response. Plasma concentration of IL-6 and compound **63** were determined 2 hours post LPS challenge. Values represent mean ± SE (n=5/group).

In vivo antitumor efficacy of compound **63** is exemplified by activity in a Kasumi-1 AML mouse xenograft model shown in Figure 7. Compound **63** was dosed orally QD at 1 mg/kg for 25 days and achieved 99% tumor growth inhibition (TGI) with acceptable tolerability (weight loss ≤10%). For comparison a representative therapy for AML, 5-azacitidine, achieved 76% TGI when administered at its MTD (IV Q7d, 8 mg/kg). An estimate of an efficacious exposure target for compound **63** can be determined by adjusting the cellular antiproliferative potency (EC_{50} of 0.0021 µM) for protein binding (98%), resulting in an exposure target of 0.10 µM. Based on plasma exposure values obtained in a pharmacokinetic study in non-tumor bearing animals, the plasma concentration target was achieved for approximately 12 hours/day in the efficacy study (Supporting Information, Figure S7). The robust antitumor activity achieved with compound **63** at the targeted plasma concentration is in agreement with the activity in the LPS-induced cytokine biomarker study and strongly supports on-target inhibition. The breadth of activity of **63** dosed orally QD at doses ranging from 1-2 mg/kg over 14-28 days against both

heme and solid tumors has been reported elsewhere,[26,28] indicating that BET bromodomain inhibitor **63** has the potential for utility in a wide range of oncology indications.

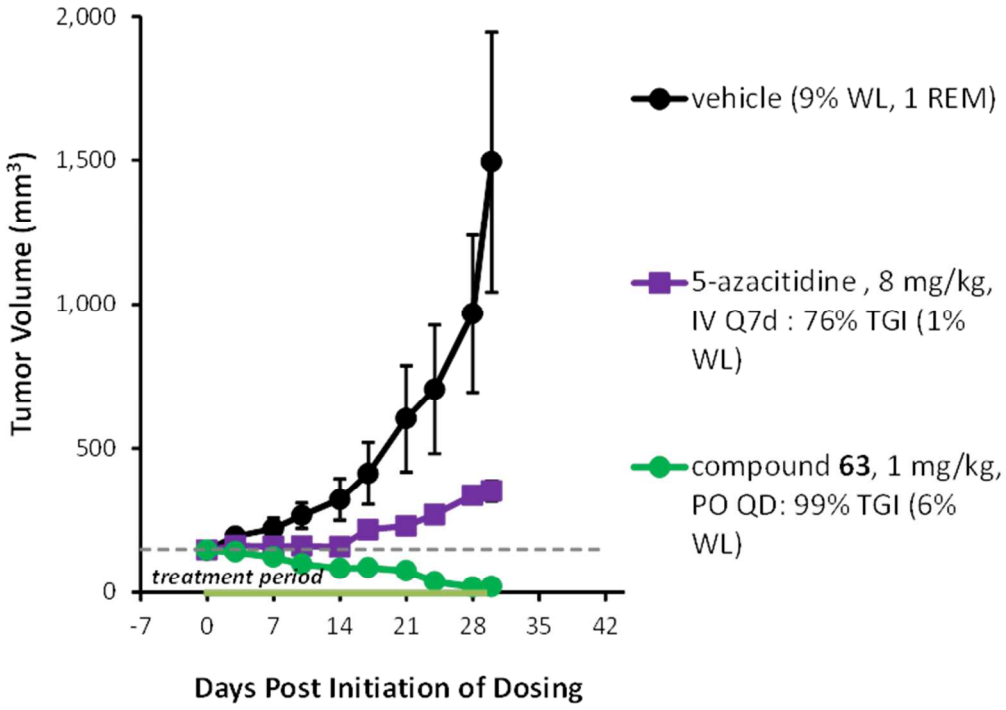

Figure 7. Kasumi-1 mouse xenograft study with compound **63**; Values represent mean ± SE (n=8/group), WL: maximum mean weight loss. REM: removed from study due to morbidity.

In addition to the evaluation of efficacy, further characterization of **63** across species also demonstrated desirable PK profiles (Table 6) supporting the choice of **63** as a clinical candidate. Indeed,

in an ongoing clinical trial[16a] where safety, tolerability, and human PK for **63** were evaluated in subjects with cancer, a prolonged half-life of 25 hours following oral administration of 1 mg (n = 3) was observed, reflecting the excellent metabolic stability observed both in vitro (microsome and hepatocyte) and in vivo (IV CLp). The observed human PK profile (1 mg oral dose) supports once daily dosing for **63** as a therapeutic agent.

Table 6. Mean PK parameters for 63 across species.

Parameter	Mouse	Rat	Dog	Monkey	Human
Microsome CL_{int}[a] (L/hr/kg)	8.3	4.0	3.1	2.3	< 1.5
Hepatocyte CL_{int}[a] (L/hr/kg)	3.5	4.0	2.1	3.1	0.87
IV CL_p[a] (L/hr/kg)	0.5	0.6	0.19	0.33	0.14[b]
F (%)	68	65	41	33	50[c]
PO CLp/F (L/hr)	-	-	-	-	5.03
$t_{1/2}$ (hr)	2.7	2.6	5.8	4.4	25.1

[a]Not corrected for protein binding as no species difference in protein binding was observed

[b]Estimated IV CLp based on observed PO CLp/F and estimated F (%)

[c]Estimated F (%) based on observed F (%) from preclinical species

Direct binding of compound **63** to BRD4 bromodomains I and II was tested by isothermal titration calorimetry (ITC). Compound **63** binds to both domains tightly with Kd < 10 nM (Supporting Information, Figure S8). The selectivity of compound **63** across both the BET family and a set of bromodomain-containing proteins was also examined. Compound **63** binds to the tandem domains of BRD2, BRD4, and BRDT with similar affinities (Table 7), although binding of compound **63** to the tandem domain of BRD3 is approximately 10-fold weaker. In addition, examination of the activity of compound **63** against a set of bromodomain-containing proteins revealed moderate activity against EP300 (K_d = 87 nM, 54-fold selectivity vs. BRD4) and potential weak activity against SMARCA4 (70%

inhibition at 1 μM), but displayed K_d > 1 μM for 18 other bromodomain proteins that were examined (Table S4, Supporting Information).

Table 7. Comparative binding data for 63 within BET family (K_i in nM)

	BRD2	BRD3	BRD4	BRDT
ID	BDI-BDII	BDI-BDII	BDI-BDII	BDI-BDII
	G73-A560	P24-P416	K57-K550	N21-P380
63	1.0	12.2	1.5	2.2

In order to evaluate potential off-target interactions, compound **63** was evaluated in a Cerep panel screen (Cerep, http://www.cerep.fr) against 79 molecular targets, including receptors and enzymes, measured at 10 μM. Compound **63** displayed excellent selectivity, as only three targets displayed > 80% displacement of control-specific binding (A1 @ 97%, A2A @ 87%, and peripheral benzodiazepine @ 86%, see Table S5 in the Supporting Information). Follow-up studies were conducted to establish whether the binding of compound **63** to these receptors modulated their function. Compound **63** only modulated the functional activity of the A2B receptor (IC_{50} = 2.6 μM, antagonist activity) and the peripheral benzodiazepine receptor (IC_{50} = 0.80 μM), thus providing at least a 500-fold window vs. BRD4 tandem domain binding.

The metabolism profile of compound **63** was also examined. A rat mass balance study using radiolabeled-**63** demonstrated that **63** is primarily eliminated via metabolism (76% of the dose administered). In vitro studies further identified CYP3A4/5 as the major metabolic enzymes that contribute to > 60% of the metabolism of **63** in human hepatocytes, which suggest it may carry victim liability upon co-administration with strong CYP3A inhibitors or inducers in humans. From a perpetrator perspective, **63** does not appear to carry significant liabilities at its efficacious concentration based on in vitro characterization.

▪ CONCLUSIONS

The structure-based design of the pyrrolopyridone BET family bromodomain inhibitor **63** has been described. Incorporation of a pyrrole moiety with the original pyridone core enabled a substantially more productive bidentate interaction with the crucial asparagine moiety of the BET protein and provided a concomitant boost in activity (9- to 19-fold). Examination of a range of substituents reaching off of the central aromatic ring of the core pyrrolopyridone inhibitor **19** led to the incorporation of a valuable sulfonamide moiety (compounds **24-26)** and an improvement in activity resulting from a useful interaction with a backbone protein aspartic acid residue. Finally, a metabolic pathways analysis identified the pendant unsubstituted phenylether moiety as a hotspot for metabolism, particularly in rat. Incorporation of electron-withdrawing substituents on this aromatic ring substantially reduced this problematic metabolism, and led directly to the discovery of **63**, a structurally novel BET bromodomain inhibitor with superior potency in TR-FRET binding assays and excellent activity in a wide range of cellular phenotypes. Compound **63** also displays an advantageous DMPK profile across multiple species, and demonstrates excellent exposures and a 25 h half-life in humans. Compound **63** demonstrates valuable activity in a wide range of in vivo efficacy models, and currently is under examination in Phase I clinical trials.

▪ EXPERIMENTAL SECTION

Protein expression and purification. Human BRD4 BDII (residues 352-457) and BDR4 BDI-BDII (residues 57-550) were cloned into the pET28b vector to make N-terminal His6 with thrombin cleavage site constructs. All the proteins were expressed in *E. Coli* BL21(DE3) cells and purified from the soluble fraction using a Ni-NTA column. For X-ray studies, the His6-tag was cleaved with thrombin protease and the protein was further purified using size exclusion chromatography.

BRD protein crystallization method. Human BRD4 BDII protein was concentrated to ~4 mg/mL in 10 mM Bis-Tris, pH 6.8, 100 mM NaCl, 5 mM DTT buffer. Protein was incubated with compounds at a 3:1 mM ratio of compound to protein at 4 °C for 2 h. The protein-compound complexes

were screened against SGC-1 and SGC Redwing custom screens (prepared by Rigaku) at 17 °C. Some protein-compound complexes were also screened against commercially available screens PEGRx and SaltRx (Hampton Research) at 17 °C. Vapor-diffusion sitting drops were prepared using a Mosquito liquid dispenser (TTP Labtech) in MRC 2 Well Crystallization plates (Hampton Research.) The drops contained 0.3 μL of protein and 0.3 μL of reservoir solution over wells of 40 μL of reservoir solution.

TR-FRET bromodomain binding assay. A time-resolved fluorescence resonance energy transfer (TR-FRET) assay was used to determine the affinities (K_i) of compounds for the tandem bromodomain of BRD4. Compound dilution series were prepared in DMSO via an approximately 3-fold serial dilution. Compound dilutions were added directly into white, low-volume assay plates (Perkin Elmer Proxiplate 384 Plus# 6008280) using a Labcyte Echo in conjunction with Labcyte Access and Thermo Multidrop CombinL robotics. Compounds were then suspended in eight microliters (μL) of assay buffer (20 mM sodium phosphate, pH 6.0, 50 mM NaCl, 1 mM ethylenediaminetetraacetic acid disodium salt dihydrate, 0.01% Triton X-100, 1 mM DL-dithiothreitol) containing His-tagged bromodomain, europium-conjugated anti-His antibody (Invitrogen PV5596) and Alexa-647-conjugated probe. The final concentration of 1X assay mixture contained 0.5% DMSO, 5 nM His tagged BRD4 (BDI-II_K57- K550) and 30 nM probe, and 1 nM europium-conjugated anti-His-tag antibody, and compound concentrations in the range of: 49.75 μM-0.18 nM. After a 1 h equilibration at room temperature, TR-FRET ratios were determined using an Envision multilabel plate reader (Ex 340, Em 495/520). TR-FRET data were normalized to the means of 24 no-compound controls ("high") and 8 controls containing 1 μM un-labeled probe ("low"). Percent inhibition was plotted as a function of compound concentration and the data were fit with the 4 parameter logistic equation to obtain IC_{50}s. Inhibition constants (K_i) were calculated from the IC_{50}s, probe K_d (0.021 μM) and probe concentration. The TR-FRET binding assay had a running MSR = 1.2 and Test-retest MSR = 2.1. Compound **1b** was tested as a positive control for this assay, with a determined K_i value of 77 ± 17 nM. A representative curve used for the determination of TR-FRET K_i for compound **63** is shown in the Supporting

Information (Figure S1). The synthesis of the Alexa647-conjugated probe is described in the Supporting Information.

MX-1 proliferation assay. The impact of compounds on cancer cell proliferation was determined using the triple negative breast cancer cell line MX-1 (ATCC) in a 3-day proliferation assay. MX-1 cells were maintained in RPMI 1640 medium (Sigma) supplemented with 10% FBS at 37 °C and an atmosphere of 5% CO_2. For compound testing, MX-1 cells were plated in 96-well black bottom plates at a density of 5000 cells/well in 90 µL of culture media and incubated at 37 °C for 18 h to allow cell adhesion and spreading. Compound dilution series were prepared in DMSO via a 3-fold serial dilution from 3 mM to 0.1 µM. The DMSO dilution series were then diluted 1:100 in phosphate buffered saline and 10 µL of the resulting solution were added to the appropriate wells of the MX-1 cell plate. The final compound concentrations in the wells were 3, 1, 0.3, 0.1, 0.03, 0.01, 0.003, 0.001, 0.0003 and 0.0001 µM. After the addition of compounds, the cells were incubated for an additional 72 h and the amounts of viable cells were determined using the Cell Titer Glo assay kit (Promega) according to manufacturer-suggested protocol. Luminescence readings from the Cell Titer Glo assay were normalized to the DMSO treated cells and analyzed using the GraphPad Prism software with sigmoidal curve fitting to obtain EC_{50}s. The minimum significant ratio (MSR) was determined to evaluate assay reproducibility (Eastwood et al., (2006) *J* Biomol Screen, 11: 253-261). The MX-1 cell proliferation assay had a running MSR = 1.2 and a Test-retest MSR = 4.7. Compound **1b** was tested as a positive control for this assay, with a determined EC_{50} value of 254 nM. A representative curve used for the determination of the MX-1 proliferation EC_{50} for compound **63** is shown in the Supporting Information (Figure S2)

BRD4 engagement luciferase reporter assay conditions. Target engagement in cells was measured with a luciferase reporter assay based on the contribution of BRD4 to human papilloma virus (HPV) E2-mediated transcriptional repression, where BRD4 is part of the HPV long control region (LCR) promoter repression complex with E2 and EP400. An H1299-derived cell line was generated with a stably integrated E2 expression cassette and an HPV-LCR-driven luciferase reporter. A

luciferase signal occurs only when a BET inhibitor blocks BRD4, thus providing a measure of target engagement (Figure S3). H1299 cells were engineered to stably express E2 and an HPV16-LCR luciferase reporter by dual selection in geneticin and puromycin. The H1299-E2/HPV-LCR-Luc cell line was subsequently maintained in RPMI1640 supplemented with 10% FBS (Gibco) in a humidified incubator at 37 °C, 5% CO_2. Cells were seeded for 18 h in 96-well tissue culture treated plates, and treated with serial dilution of compound for 24 h. Luciferase was measured using Bright-Glo luciferase assay (Promega) with a Victor Luminometer (Perkin Elmer). The percentage inhibition of luciferase signal was normalized to control cells treated with DMSO and IC_{50}s were calculated by nonlinear regression analysis using GraphPad PRISM software. The BRD4 engagement assay had a running MSR = 1.3 and a Test-retest MSR = 2.6. Compound **1b** was tested as a positive control for this assay, with a determined EC_{50} value of 153 nM. A representative curve used for the determination of the BRD4 Engagement EC_{50} for compound **63** is shown in the Supporting Information (Figure S4).

Synthetic Materials and Methods. Unless otherwise specified, reactions were performed under an inert atmosphere of nitrogen and monitored by thin-layer chromatography (TLC) and/or LCMS. All reagents were purchased from commercial suppliers and used as provided. 3-Mercaptopropyl-functionalized silica gel (Aldrich, catalog 538086) was routinely used to remove ionic palladium species during work up of Suzuki coupling reactions. 1,3,5,7-Tetramethyl-6-phenyl-2,4,8-trioxa-6-phosphaadamantane (Aldrich catalog 695459, CAS 97739-46-3) was a preferred ligand for Suzuki coupling reactions. Flash column chromatography was carried out on pre-packed silica gel cartridges. Reverse phase chromatography samples were purified by preparative HPLC on a Phenomenex Luna C8(2) 5 μm 100Å AXIA column (30 mm × 75 mm). A gradient of acetonitrile (A) and 0.1% trifluoroacetic acid in water (B) was used, at a flow rate of 50 mL/min (0-0.5 min 10% A, 0.5-7.0 min linear gradient 10-95% A, 7.0-10.0 min 95% A, 10.0-12.0 min linear gradient 95-10% A). Samples were

injected in 1.5 mL DMSO:methanol (1:1). A custom purification system was used, consisting of the following modules: Waters LC4000 preparative pump; Waters 996 diode-array detector; Waters 717+ autosampler; Waters SAT/IN module, Alltech Varex III evaporative light-scattering detector; Gilson 506C interface box; and two Gilson FC204 fraction collectors. The system was controlled using Waters Millennium32 software, automated using an AbbVie-developed Visual Basic application for fraction collector control and fraction tracking. Fractions were collected based upon UV signal threshold and selected fractions subsequently analyzed by flow injection analysis mass spectrometry using positive APCI ionization on a Finnigan LCQ using 70:30 methanol:10 mM NH_4OH (aq) at a flow rate of 0.8 mL/min. Loop-injection mass spectra were acquired using a Finnigan LCQ running LCQ Navigator 1.2 software and a Gilson 215 liquid handler for fraction injection controlled by an AbbVie-developed Visual Basic application. All NMR spectra were recorded on 300-500 MHz instruments as specified with chemical shifts given in ppm (δ) and are referenced to an internal standard of tetramethylsilane (δ 0.00). $^1H - {}^1H$ couplings are assumed to be first-order and peak multiplicities are reported in the usual manner. HPLC purity determinations were performed on a Waters e2695 Separation Module / Waters 2489 UV/Visible Detector. Column types and elution methods are described in the Supporting Information section. The purity of all of the biologically evaluated compounds was determined to be >95% using two separate HPLC methods, except for compound **26** (94.5% purity, method A, 95.1% purity, method B) and compound **60** (98.6% purity, method A, 93.4% purity, method B). Solvents used for HPLC analysis and sample preparation were HPLC grade.

1-Methyl-5-(2-phenoxyphenyl)pyridin-2(1H)-one (9). A mixture of 2-phenoxyphenylboronic acid (0.14 g, 0.65 mmol, 1.3 eq.), 5-bromo-1-methylpyridin-2(1H)-one (**8**, 0.094 g, 0.50 mmol), $Pd(PPh_3)_4$ (0.029 g, 0.025 mmol, 0.05 eq.), and cesium fluoride (0.23 g, 1.5 mmol, 3 eq.) in dimethoxy ethane (3 mL) and methanol (1.5 mL) was degassed and heated under microwave conditions at 120 °C for 3 h. After cooling to ambient temperature, the reaction mixture was partitioned between water and ethyl acetate. The aqueous layer was extracted with ethyl acetate three additional times. The combined

organic layers were washed with saturated aqueous sodium chloride, dried over anhydrous magnesium sulfate, filtered, and concentrated. The residue was purified by flash chromatography (silica gel, 80% ethyl acetate in heptanes) followed by reverse phase HPLC (C18, 10-70% acetonitrile in water (0.1% TFA)) to provide the title compound (0.11 g, 79%). ^{1}H NMR (500 MHz, DMSO-d_6) δ 7.91 (d, J = 2.4 Hz, 1H), 7.63 (dd, J = 9.3, 2.6 Hz, 1H), 7.48 (dd, J = 7.6, 1.8 Hz, 1H), 7.23-7.37 (m, 3H), 7.23-7.27 (m, 1H), 7.08 (t, J = 7.5 Hz, 1H), 6.92-6.98 (m, 3H), 3.44(s, 3H). MS (DCI+) m/z 278.1 $(M+H)^+$.

3-Methyl-5-(2-phenoxyphenyl)pyridin-2(1H)-one (11). 2-Phenoxyphenylboronic acid (0.072 g, 0.34 mmol), 5-bromo-3-methylpyridin-2(1H)-one (**10**, 0.060 g, 0.32 mmol), bis(triphenylphosphine)palladium(II) chloride (0.0090 g, 0.013 mmol) and 2.0 M aqueous sodium carbonate (0.64 mL, 1.3 mmol) were combined in 1,2-dimethoxyethane (1.6 mL) and ethanol (1.6 mL), sparged with nitrogen for 15 min and heated under microwave conditions at 120 ºC for 30 min. The reaction mixture was partitioned between ethyl acetate and water. The ethyl acetate layer was washed with saturated aqueous sodium chloride, dried over anhydrous sodium sulfate, filtered, and concentrated. Purification by reverse phase HPLC (C18, 0-100% CH_3CN/water (0.1% TFA)) afforded the title compound as the trifluoroacetic acid salt (0.020 g, 23%). ^{1}H NMR (300 MHz, DMSO-d_6) δ 11.60 (s, 1H), 6.75 - 7.63 (m, 11H), 1.97 (m, 3 H). MS (APCI+) m/z 278 $(M+H)^+$.

3-Amino-1-methyl-5-(2-phenoxyphenyl)pyridin-2(1H)-one (13). A mixture of 3-amino-5-bromo-1-methylpyridin-2(1H)-one (**12**, 0.10 g, 0.50 mmol), (2-phenoxyphenyl)boronic acid (0.21 g, 1.0 mmol), $Pd(PPh_3)_4$ (0.029 g, 0.025 mmol), and cesium fluoride (0.23 g, 1.5 mmol) in DME (2 mL) and MeOH (1 mL) was heated at 120 °C under microwave conditions for 40 min. The reaction mixture was partitioned between water and ethyl acetate. The aqueous layer was extracted with additional ethyl acetate three times. The combined organic layers were washed with brine, dried over anhydrous magnesium sulfate, filtered, and concentrated. The residue was purified by flash column chromatography (silica gel eluting, 90% ethyl acetate in hexanes) to give the title compound (0.12 g, 82%). ^{1}H NMR (400 MHz, DMSO-d_6) δ 7.63 – 7.55 (m, 2H), 7.53 (dd, J = 6.7, 3.1 Hz, 1H), 7.39 (dd, J

= 7.6, 1.8 Hz, 1H), 7.29 (t, *J* = 7.9 Hz, 2H), 7.23 – 7.15 (m, 2H), 7.03 (t, *J* = 7.4 Hz, 1H), 6.92 (dd, *J* = 8.1, 1.2 Hz, 1H), 6.87 (d, *J* = 8.2 Hz, 2H), 6.84 (d, *J* = 2.3 Hz, 1H), 3.43 (s, 1H). MS (ESI+) m/z 293.2 $(M+H)^+$.

(E)-2-(5-Bromo-2-methoxy-3-nitropyridin-4-yl)-N,N-dimethylethenamine (14). 5-Bromo-2-methoxy-4-methyl-3-nitropyridine (15.0 g, 60.7 mmol) was dissolved in dimethylformamide (300 mL), and lithium methanolate (6.07 mL, 6.07 mmol, 1 M) was added. The reaction mixture was heated to 100 °C. To this mixture was added 1,1-dimethoxy-N,N-dimethylmethanamine (64.5 mL, 486 mmol) over 10 min. The reaction mixture was stirred at 95 °C for 16 h. The reaction mixture was cooled to ambient temperature and water was added carefully (300 mL, exothermic). The resulting precipitate was collected by vacuum filtration, washed with water, and dried to provide the title compound (13.9 g, 76%). ^{1}H NMR (300 MHz, DMSO-d_6) δ 8.25 (s, 1H), 7.05 (d, *J* = 13.9 Hz, 1H), 4.80 (d, *J* = 13.5 Hz, 1H), 3.88 (m, 3 H), 2.91 (s, 6H). MS (ESI+) m/z 302.0 $(M+H)^+$.

4-Bromo-7-methoxy-1H-pyrrolo[2,3-c]pyridine (15). Compound **14** (13.9 g, 45.8 mmol) and ethyl acetate (150 mL) were added to Ra-Ni 2800 (pre-washed with ethanol) water slurry (6.9 g, 120 mmol) in a stainless steel pressure bottle and stirred for 30 min at 30 psi at ambient temperature. The reaction mixture was filtered, and concentrated. The residue was triturated with dichloromethane, and the solid filtered to provide the title compound (5.82 g). The mother liquor was evaporated and the residue triturated again with dichloromethane and filtered to provide an additional 1.63 g of the title compound. Total yield=7.45 g, 72%. ^{1}H NMR (500 MHz, DMSO-d_6) δ 12.16 (s, 1H), 7.76 (s, 1H), 7.56 (d, *J* = 3.1 Hz, 1H), 6.44 (d, *J* = 3.1 Hz, 1H), 4.02 (s, 3 H). MS (ESI+) m/z 226.8 $(M+H)^+$.

4-Bromo-7-methoxy-1-tosyl-1H-pyrrolo[2,3-c]pyridine (16). A solution of **15** (7.42 g, 32.7 mmol) in dimethylformamide (235 mL) was stirred at ambient temperature. To this solution was added sodium hydride (1.18 g, 1.96 g of 60% dispersion in oil, 49.0 mmol), and the reaction mixture was stirred for 10 min. *P*-toluenesulfonyl chloride (9.35 g, 49.0 mmol) was then added portion-wise, and the mixture was stirred at ambient temperature under nitrogen for 16 h. The reaction mixture was quenched

carefully with water and the resulting beige solid collected by vacuum filtration on a Buchner funnel and washed with water. The solid was collected and dried in a vacuum oven at 50 °C to provide the title compound (12.4 g, 100%). ^{1}H NMR (300 MHz, DMSO-d_6) δ 8.18 (d, J = 3.7 Hz, 1H), 8.00 (s, 1H), 7.85 (d, J = 8.5 Hz, 2H), 7.46 (d, J = 8.1 Hz, 2H), 6.81 (d, J = 3.7 Hz, 1H), 3.82 (s, 3H), 2.38 (s, 3H). MS (ESI+) m/z 382.9 $(M+H)^+$.

4-Bromo-1-tosyl-1H-pyrrolo[2,3-c]pyridin-7(6H)-one (17). A solution of **16** (12.4 g, 32.6 mmol) in 1,4-dioxane (140 mL) was stirred at ambient temperature. To this solution was added 4 M HCl in 1,4-dioxane (140 mL). The reaction mixture was stirred at 40 °C for 16 h. The reaction mixture was cooled to ambient temperature and concentrated. The residue was triturated with diethyl ether, filtered, and rinsed with additional diethyl ether and dried to provide the title compound (11.2 g, 94%) as a beige solid. ^{1}H NMR (500 MHz, DMSO-d_6) δ 11.51 (s, 1H), 8.05 (d, J = 3.7 Hz, 1H), 7.95 (d, J = 8.5 Hz, 2H), 7.41 (d, J = 7.9 Hz, 2H), 7.36 (s, 1H), 6.60 (d, J = 3.4 Hz, 1H), 2.37 (s, 3H). MS (ESI+) m/z 369.1 $(M+H)^+$.

4-Bromo-6-methyl-1-tosyl-1H-pyrrolo[2,3-c]pyridin-7(6H)-one (18). Sodium hydride (1.46 g of a 60% oil dispersion, 36.5 mmol) was added to a stirring solution of compound **17** (11.2 g, 30.4 mmol) in dimethylformamide (217 mL) under nitrogen. After 30 min, iodomethane (2.27 mL, 36.5 mmol) was added and the solution was stirred at ambient temperature for 3 h. Upon addition of water (250 mL), a precipitate formed. The precipitate was collected by vacuum filtration, rinsed with water (50 mL) and dried in a vacuum oven at 55 °C for 16 h to provide the title compound (11.2 g, 96%). ^{1}H NMR (300 MHz, DMSO-d_6) δ 8.05 (d, J = 3.4 Hz, 1H), 7.95 (d, J = 8.5 Hz, 2H), 7.80 (s, 1H), 7.42 (d, J = 8.1 Hz, 2H), 6.59 (d, J = 3.4 Hz, 1H), 3.39 (s, 3H), 2.38 (s, 3H). MS (ESI+) m/z 382.9 $(M+H)^+$.

6-Methyl-4-(2-phenoxyphenyl)-1,6-dihydro-7H-pyrrolo[2,3-c]pyridin-7-one (19). A mixture of compound **18** (152 mg, 0.40 mmol), 2-phenoxyphenylboronic acid (0.111 g, 0.520 mmol), $Pd(PPh_3)_4$ (0.023 g, 5 mol%) and cesium fluoride (0.18 g, 1.2 mmol) in DME (3 mL) and methanol (1.5 mL) was

heated under microwave conditions (120 ºC, 30 min). To this mixture was added potassium carbonate (0.055 g, 0.40 mmol) and water (1 mL) and the reaction mixture was reheated in the microwave oven at 120 ºC for an additional 2 h. The organic layer was separated and purified by flash chromatography (silica gel, ethyl acetate). The resulting material was triturated with acetone and filtered to provide the title compound (0.075 g, 59%). ^{1}H NMR (500 MHz, DMSO-d_6) δ 11.98 (s, 1H), 7.50 (dd, J = 7.5, 1.7 Hz, 1H), 7.36-7.40 (m, 1H), 7.24-7.30 (m, 5H), 6.99-7.04 (m, 2H), 6.88 (d, J = 7.6 Hz, 2H), 6.21-6.23 (m, 1H), 3.50 (s, 3H). MS (ESI+) m/z 317 $(M+H)^+$.

4-(2-Fluoro-5-nitrophenyl)-6-methyl-1-tosyl-1H-pyrrolo[2,3-c]pyridin-7(6H)-one (21). Compound **18** (0.687 g, 1.80 mmol), 2-fluoro-5-nitrophenylboronic acid (**20**, 0.500 g, 2.70 mmol), $Pd(PPh_3)_4$ (0.104 g, 0.090 mmol), and 2.0 M aqueous sodium carbonate (2.70 mL, 5.41 mmol) were combined in DME (7 mL) and water (7 mL) in a 20 mL microwave tube, sealed, sparged with nitrogen and heated under microwave conditions at 120 ºC for 30 min. The mixture was partitioned between ethyl acetate and water. The organic layer was washed with saturated aqueous sodium chloride, dried over anhydrous sodium sulfate, filtered, and concentrated. The crude product was purified by flash chromatography (silica gel, 0-100% ethyl acetate in hexanes) to provide the title compound (0.41 g, 52%). ^{1}H NMR (300 MHz, DMSO-d_6) δ 8.42 – 8.32 (m, 1H), 8.06 (d, J = 3.5 Hz, 1H), 8.03 – 7.98 (m, 1H), 7.78 (d, J = 0.5 Hz, 1H), 7.74 – 7.63 (m, 1H), 7.51 – 7.41 (m, 1H), 6.55 (dd, J = 3.6, 3.0 Hz, 1H), 3.50 (s, 2H), 2.42 (s, 2H). MS (ESI+) m/z 442.1 $(M+H)^+$.

6-Methyl-4-(5-nitro-2-phenoxyphenyl)-1,6-dihydro-7H-pyrrolo[2,3-c]pyridin-7-one (22). Phenol (0.094 g, 1.0 mmol), compound **21** (0.40 g, 0.91 mmol) and cesium carbonate (0.33 g, 1.0 mmol) were combined in DMSO (4.5 mL) and heated at 100 ºC for 2 h. The reaction mixture was partitioned between ethyl acetate and water and the pH was adjusted to 7. The organic layer was washed with saturated aqueous sodium chloride, dried over anhydrous sodium sulfate, filtered, and concentrated. Purification by flash chromatography (silica gel, 0-4% methanol in dichloromethane) afforded the title compound (0.28 g, 84%). ^{1}H NMR (300 MHz, DMSO-d_6) δ 12.07-12.11 (m, 1H), 8.32 (d, J = 2.8 Hz,

1H), 8.22 (dd, J = 9.1, 2.8 Hz, 1H), 7.40-7.49 (m, 3H), 7.21-7.32 (m, 2H), 7.16 (d, J = 7.5 Hz, 2H), 6.98 (d, J = 9.1 Hz, 1H), 6.28-6.34 (m, 1H), 3.57 (s, 3H). MS (ESI+) m/z 362 $[M+H]^+$.

4-(5-Amino-2-phenoxyphenyl)-6-methyl-1,6-dihydro-7H-pyrrolo[2,3-c]pyridin-7-one (23). Compound **22** (0.25 g, 0.69 mmol), iron powder (0.19 g, 3.5 mmol), and ammonium chloride (0.056 g, 1.0 mmol) were combined in THF (6 mL), ethanol (6 mL) and water (2 mL). The mixture was heated at 95 ºC with vigorous stirring for 1.5 h. The reaction mixture was cooled to ambient temperature and filtered through a plug of Celite to remove the solids. The plug was rinsed repeatedly with methanol and THF. The filtrate was concentrated and the residue partitioned between ethyl acetate and water. The ethyl acetate layer was washed with saturated aqueous sodium chloride, dried over anhydrous sodium sulfate, filtered, and concentrated. The residue was purified by flash chromatography (silica gel, 1-4% methanol in dichloromethane) to afford the title compound (0.21 g, 82%). ^{1}H NMR (300 MHz, DMSO-d_6) δ 11.91 (s, 1H), 7.24 (t, J = 2.7 Hz, 1H), 7.11-7.19 (m, 3H), 6.80-6.88 (m, 2H), 6.74 (d, J = 2.7 Hz, 1H), 6.68 (d, J = 7.8 Hz, 2H), 6.59 (dd, J = 8.5, 2.7 Hz, 1H), 6.22-6.25 (m, 1H), 5.07 (s, 2H), 3.43 (s, 3H). MS (ESI+) m/z 362 $[M+H]^+$.

N-[3-(6-Methyl-7-oxo-6,7-dihydro-1H-pyrrolo[2,3-c]pyridin-4-yl)-4 phenoxyphenyl]methane-sulfonamide (24). To a solution of compound **23** (0.125 g, 0.377 mmol) and triethylamine (0.13 mL, 0.94 mmol) in dichloromethane (3.0 mL) was added dropwise methanesulfonyl chloride (0.064 mL, 0.83 mmol). The reaction mixture was stirred for 2 h and then concentrated. The residue was dissolved in a mixture of 1,4-dioxane (5 mL) and 1 M aqueous sodium hydroxide (2 mL) and heated for 1 h at 90 ºC. The reaction mixture was cooled and diluted with ethyl acetate, brought to pH 7 with 1 M HCl and partitioned. The organic layer was washed with saturated aqueous sodium chloride, dried over anhydrous sodium sulfate, filtered, and concentrated. The residue was purified by flash chromatography (silica gel, 0-4% methanol in dichloromethane) to afford the title compound (0.119 g, 77%). ^{1}H NMR (300 MHz, DMSO-d_6) δ 12.01 (s, 1H), 9.72 (s, 1H), 7.39 (d, J = 2.7 Hz, 1H),

7.20-7.29 (m, 5H), 7.04 (d, J = 8.8 Hz, 1H), 6.99 (t, J = 7.3 Hz, 1H), 6.85 (d, J = 7.5 Hz, 2H), 6.23-6.30 (m, 1H), 3.48 (s, 3H), 3.02 (s, 3H). MS (ESI+) m/z 410 $[M+H]^+$.

N-[3-(6-Methyl-7-oxo-6,7-dihydro-1H-pyrrolo[2,3-c]pyridin-4-yl)-4 phenoxyphenyl]methane-sulfonamide (24) via the approach outlined in Scheme 5. Compound **28** (7.0 g, 16 mmol), compound **37** (5.87 g, 17.2 mmol), tris(dibenzylideneacetone)dipalladium(0) (0.374 g, 0.409 mmol), 1,3,5,7-tetramethyl-6-phenyl-2,4,8-trioxa-6-phosphaadamante (0.239 g, 0.817 mmol) and potassium phosphate (10.8 g, 50.7 mmol) were combined in a 20 mL sealed tube and sparged with argon for 30 min. Meanwhile a solution of 4:1 1,4-dioxane/water (10 mL total volume) was sparged with nitrogen for 30 min and transferred by syringe into the reaction vessel under argon. The mixture was stirred at 60 °C for 2 h. The mixture was cooled and partitioned between ethyl acetate and water. The organic layer was washed with saturated aqueous sodium chloride, dried over anhydrous sodium sulfate, treated with mercaptopropyl silica gel for 45 min, filtered, and concentrated. Purification by flash chromatography (silica gel, 20-100% ethyl acetate in hexanes) afforded an amorphous solid that was triturated in refluxing ethyl acetate for 30 min, cooled to ambient temperature, and filtered to afford the title compound (7.3 g, 79%). ^{1}H NMR (300 MHz, DMSO-d_6) δ 9.72 (s, 1H), 7.97 – 7.87 (m, 3H), 7.47 (s, 1H), 7.44 – 7.37 (m, 2H), 7.29 – 7.16 (m, 4H), 7.05 – 6.94 (m, 2H), 6.85 – 6.77 (m, 2H), 6.51 (d, J = 3.5 Hz, 1H), 3.37 (s, 3H), 3.01 (s, 3H), 2.37 (s, 3H). MS (ESI+) m/z 564.3 $(M+H)^+$. A portion of this material (1.13 g, 2.0 mmol), potassium hydroxide (1.82 g, 52.5 mmol), and cetyltrimethylammonium bromide (0.036 g, 0.10 mmol) were combined in THF (15 mL) and water (5 mL) and heated at 100 °C for 14 h. The reaction mixture was partitioned between equal volumes of ethyl acetate and water and the pH was adjusted to 7 by careful addition of concentrated HCl. The organic layer was separated, washed three times with saturated aqueous sodium chloride, dried over anhydrous sodium sulfate, and concentrated. Purification by trituration in dichloromethane afforded the title compound (0.76 g, 93%). The spectral data for this material matched the data obtained for compound **24** generated according to Scheme 3.

N-[3-(6-methyl-7-oxo-6,7-dihydro-1H-pyrrolo[2,3-c]pyridin-4-yl)-4-phenoxyphenyl]ethanesulfonamide (25). To a solution of compound **23** (0.055 g, 0.17 mmol) and triethylamine (0.069 mL, 0.50 mmol) in dichloromethane (1.2 mL) was added dropwise methanesulfonyl chloride (0.047 mL, 0.064 g, 0.50 mmol). The reaction mixture was stirred for 1 h and then concentrated. The reaction mixture was neutralized by the addition of saturated aqueous ammonium chloride to pH 8 and extracted with ethyl acetate. The organic layer was washed with saturated aqueous sodium chloride, dried over anhydrous magnesium sulfate, filtered, and concentrated. The residue was purified by reverse phase HPLC (C18, 0-100 % CH_3CN/water (0.1% TFA)) to afford the title compound (0.032 g, 45%). ^{1}H NMR (300 MHz, DMSO-d_6) δ 12.02 (bs, 1H), 9.79 (s, 1H), 7.40 (d, J = 2.7 Hz, 1H), 7.31-7.18 (m, 5H), 7.07-6.95 (m, 2H), 6.88-6.80 (m, 2H), 6.26 (t, J = 2.3 Hz, 1H), 3.48 (s, 3H), 3.13 (q, J = 7.3 Hz, 2H), 1.24 (t, J = 7.3 Hz, 3H). MS (ESI+) m/z 424.2 $(M+H)^+$.

2,2,2-Trifluoro-N-[3-(6-methyl-7-oxo-6,7-dihydro-1H-pyrrolo[2,3-c]pyridin-4-yl)-4-phenoxyphenyl]ethanesulfonamide (26). To a solution of compound **23** (0.050 g, 0.15 mmol) and triethylamine (0.038 g, 0.053 mL, 0.38 mmol) in dichloromethane (1 mL) was added dropwise 2,2,2-trifluoroethanesulfonyl chloride (0.036 g, 0.20 mmol). The reaction mixture was stirred for 1 h and then concentrated. The residue was purified by flash chromatography (silica gel, 0-5% methanol in dichloromethane) to afford the title compound (0.050 g, 68%). ^{1}H NMR (300 MHz, DMSO-d_6) δ 12.02 (s, 1H), 10.43 (s, 1H), 7.40 (d, J = 2.8 Hz, 1H), 7.20-7.31 (m, 5H), 6.95-7.07 (m, 2H), 6.86 (d, J = 7.5 Hz, 2H), 6.28 (t, J = 2.4 Hz, 1H), 4.55 (q, J = 9.9 Hz, 2H) 3.49 (s, 3H). MS (APCI+) m/z 478 $[M+H]^+$.

N,N-dimethyl-N'-[3-(6-methyl-7-oxo-6,7-dihydro-1H-pyrrolo[2,3-c]pyridin-4-yl)-4-phenoxyphenyl]sulfuric diamide (27). To a solution of compound **23** (0.055 g, 0.17 mmol) and cesium carbonate (0.081 g, 0.25 mmol) in dimethylformamide (1.2 mL) was added dimethylsulfamoyl chloride (0.026 mg, 0.020 mL, 0.18 mmol). The reaction mixture was heated at 80 ºC for 1 h in a microwave reactor and then cooled to ambient temperature. The reaction mixture was partitioned

between ethyl acetate and saturated aqueous sodium chloride, and the organic layer was dried over anhydrous magnesium sulfate, filtered, and evaporated. The residue was purified by reverse phase HPLC (C18, 10-80 % CH_3CN/water (0.1% TFA)) to afford the title compound (0.0082 g, 11%). ^{1}H NMR (300 MHz, DMSO-d_6) δ 12.04-12.00 (m, 1H), 9.91 (s, 1H), 7.40 (d, J = 2.7 Hz, 1H), 7.31-7.17 (m, 5H), 7.06-6.93 (m, 2H), 6.85-6.78 (m, 2H), 6.28-6.23 (m, 1H), 3.48 (s, 3H), 2.74 (s, 6H). MS (ESI+) m/z 439.1 $(M+H)^+$.

6-Methyl-4-(4,4,5,5-tetramethyl-1,3,2-dioxaborolan-2-yl)-1-tosyl-1H-pyrrolo[2,3-c]pyridin-7(6H)-one (28). Compound **18** (6.55 g, 17.2 mmol), 4,4,4',4',5,5,5',5'-octamethyl-2,2'-bi(1,3,2-dioxaborolane) (8.73 g, 34.4 mmol), potassium acetate (3.71 g, 37.8 mmol), tris(dibenzylideneacetone)dipalladium(0) (0.393 g, 0.430 mmol) and 2-dicyclohexylphosphino-2',4',6'-triisopropylbiphenyl (X-PHOS, 0.819 g, 1.72 mmol) were combined and sparged with argon for 1 h with stirring. 1,4-Dioxane (86 mL) was sparged with nitrogen for 1 h, transferred via cannula under nitrogen to the solid components, and the mixture was heated under argon at 80 °C for 5 h. The reaction mixture was cooled to ambient temperature, partitioned between ethyl acetate and water, and filtered through Celite. The ethyl acetate layer was washed twice with saturated aqueous sodium chloride, dried over anhydrous sodium sulfate, filtered, and concentrated. The residue was purified by flash chromatography (silica gel, 25-80% ethyl acetate in hexane). The resulting material from chromatography was triturated with a minimal amount of hexanes (30 mL) and the particulate solid was collected by filtration, rinsed with a minimal amount of hexanes and dried to constant mass to afford the title compound (5.4 g, 73%). ^{1}H NMR (300 MHz, DMSO-d_6) δ 7.96 (d, J = 3.4 Hz, 1H), 7.93 – 7.85 (m, 2H), 7.70 (s, 1H), 7.43 – 7.35 (m, 2H), 6.80 (d, J = 3.4 Hz, 1H), 3.42 (s, 3H), 2.36 (s, 3H), 1.28 (s, 12H). MS (ESI+) m/z 428.8 $(M+H)^+$.

3-Bromo-5-nitro-2-phenoxypyridine (30). Phenol (0.416 g, 4.42 mmol), 3-bromo-2-chloro-5-nitropyridine (**29**, 1.00 g, 4.21 mmol) and cesium carbonate (1.37 g, 4.21 mmol) were combined in DMSO (8 mL) and heated at 80 °C for 30 min. The reaction mixture was cooled and partitioned between

ethyl acetate and water. The organic layer was washed with saturated aqueous sodium chloride, dried over anhydrous sodium sulfate, filtered, and concentrated. Purification of the residue by flash chromatography (silica gel, 0-30% ethyl acetate in hexanes) afforded the title compound (1.13 g, 91%). ^{1}H NMR (300 MHz, DMSO-d_6) δ 8.98 – 8.94 (m, 2H), 7.48 (td, J = 1.2, 0.7 Hz, 2H), 7.27 – 7.24 (m, 2H), 7.24 – 7.21 (m, 1H).

6-Methyl-4-(5-nitro-2-phenoxypyridin-3-yl)-1-tosyl-1H-pyrrolo[2,3-c]pyridin-7(6H)-one (31). Compound **28** (0.10 g, 0.23 mmol), compound **30** (0.069 g, 0.23 mmol), tris(dibenzylideneacetone)dipalladium(0) (5.34 mg, 5.84 μmol), 1,3,5,7-tetramethyl-6-phenyl-2,4,8-trioxa-6-phosphaadamante (3.4 mg, 0.012 mmol) and potassium phosphate (0.104 g, 0.490 mmol) were combined and sparged with argon for 15 min. Meanwhile, a solution of 4:1 1,4-dioxane/water (2 mL total volume) was sparged with nitrogen for 15 min and transferred by syringe into the reaction vessel under argon. The reaction mixture was stirred at 60 ºC for 16 h and cooled to ambient temperature. The reaction mixture was diluted into ethyl acetate and warmed to dissolve the solids. Water was then added and the mixture was filtered through a plug of Celite to remove solid Pd. The Celite pad was rinsed thoroughly with hot ethyl acetate. The filtrate layers were separated and the ethyl acetate layer was washed with brine, dried over anhydrous sodium sulfate, treated with mercaptopropyl silica for 30 min, filtered, and concentrated to give the title compound (0.121 g, quant.). ^{1}H NMR (300 MHz, DMSO-d_6) δ 9.06 (d, J = 2.8 Hz, 1H), 8.71 (d, J = 2.8 Hz, 1H), 7.78 (s, 1H), 7.42 (m, 4H), 7.26 – 7.20 (m, 5H), 6.74 (d, J = 3.5 Hz, 1H), 6.63 (d, J = 3.5 Hz, 1H), 3.48 (s, 3H), 2.37 (s, 3H).

4-(5-Amino-2-phenoxypyridin-3-yl)-6-methyl-1-tosyl-1H-pyrrolo[2,3-c]pyridin-7(6H)-one (32). Compound **31** (0.12 g, 0.23 mmol), iron powder (0.065 g, 1.2 mmol), and ammonium chloride (0.019 g, 0.35 mmol) were combined in THF (4 mL), ethanol (4 mL) and water (1.3 mL). The mixture was heated at 100 ºC with vigorous stirring for 1 h. The reaction mixture was cooled to ambient temperature and filtered through a plug of Celite to remove the solids. The plug was rinsed repeatedly with methanol. The filtrate was concentrated and the residue partitioned between ethyl acetate and

water. The ethyl acetate layer was washed with saturated aqueous sodium chloride, dried over anhydrous sodium sulfate, filtered, and concentrated to afford the title compound (0.11 g, quant yield). MS (ESI+) m/z 487.5 $(M+H)^+$.

N-[5-(6-Methyl-7-oxo-6,7-dihydro-1H-pyrrolo[2,3-c]pyridin-4-yl)-6-phenoxypyridin-3-yl]methanesulfonamide (33). To compound **32** (0.113 g, 0.232 mmol) and triethylamine (0.059 g, 0.081 mL, 0.94 mmol) in dichloromethane (2.3 mL) was added dropwise methanesulfonyl chloride (0.061 g, 0.041 mL, 0.53 mmol). The reaction mixture was stirred for 1 h at ambient temperature and then concentrated. The residue was dissolved in a mixture of 1,4-dioxane (4 mL) and 1 M aqueous sodium hydroxide (3 mL) and heated for 2 h at 90 ºC. The reaction mixture was cooled and diluted with water and ethyl acetate and brought to pH 7 with 1 M HCl. The organic layer was washed with saturated aqueous sodium chloride, dried over anhydrous sodium sulfate, filtered, and concentrated. The residue was purified by flash chromatography (silica gel, 1-4% methanol in dichloromethane) to afford the title compound (0.119 g, 77%). ^{1}H NMR (300 MHz, DMSO-d_6) δ 12.11 (s, 1H), 9.79 (s, 1H), 7.96 (d, J = 2.4 Hz, 1H), 7.78 (d, J = 2.8 Hz, 1H), 7.48 (s, 1H), 7.28-7.41 (m, 3H), 7.16 (t, J = 7.5 Hz, 1H), 7.10 (d, J = 7.5 Hz, 2H), 6.28-6.36 (m, 1H), 3.05 (s, 3H) 3.57 (s, 3H). MS (ESI+) m/z 411.0 $(M+H)^+$.

2-Bromo-4-nitro-1-phenoxybenzene (35). 2-Bromo-1-fluoro-4-nitrobenzene (**34**, 2.5 g, 11.4 mmol), phenol (1.28 g, 13.6 mmol), and cesium carbonate (4.44 g, 13.6 mmol) were combined in DMSO (140 mL) and heated to 110 °C for 1 h. The reaction mixture was partitioned between ethyl acetate and saturated aqueous sodium chloride, and the separated aqueous phase was extracted with ethyl acetate. The combined organics were washed with saturated aqueous sodium chloride, dried over anhydrous magnesium sulfate, filtered, and concentrated to afford the title compound (3.43 g, quant. yield). ^{1}H NMR (300 MHz, Chloroform-d) δ 8.58 (d, J = 2.7 Hz, 1H), 8.12 (dd, J = 9.1, 2.7 Hz, 1H), 7.53 – 7.43 (m, 2H), 7.34 – 7.30 (m, 1H), 7.15 – 7.09 (m, 2H), 6.86 (d, J = 9.1 Hz, 1H).

3-Bromo-4-phenoxyaniline (36). Compound **35** (2.94 g, 10.0 mmol), iron powder (2.79 g, 50.0 mmol), and ammonium chloride (0.802 g, 15.0 mmol) were combined in ethanol (24 mL), THF (24

mL), and water (8 mL), and heated at 95 °C for 1.5 h. The reaction mixture was cooled to just below reflux and vacuum filtered through diatomaceous earth. The filter cake was washed repeatedly with ethanol and THF, and the filtrate concentrated under reduced pressure. The residue was partitioned between saturated aqueous sodium chloride and ethyl acetate, and the aqueous phase was extracted with additional ethyl acetate. The combined organics were washed with saturated aqueous sodium chloride, dried over anhydrous sodium sulfate, filtered, and concentrated to afford the title compound (2.56 g, 97%). ^{1}H NMR (300 MHz, DMSO-d_6) δ 7.36 – 7.28 (m, 2H), 7.02 (ddt, J = 7.8, 7.0, 1.1 Hz, 1H), 6.91 (d, J = 1.9 Hz, 1H), 6.90 (d, J = 4.2 Hz, 1H), 6.84 – 6.79 (m, 2H), 6.62 (dd, J = 8.6, 2.6 Hz, 1H), 5.33 (bs, 2H).

N-(3-Bromo-4-phenoxyphenyl)methanesulfonamide (37). Compound **36** (2.86 g, 10.8 mmol) and triethylamine (6.03 mL, 43.3 mmol) were stirred in dichloromethane (48.1 mL) at ambient temperature. Methanesulfonyl chloride (2.53 mL, 32.4 mmol) was added dropwise and the solution was stirred at ambient temperature for 1 h. The reaction mixture was concentrated under reduced pressure, 1,4-dioxane (24 mL) and sodium hydroxide solution (10% w/v, 12 mL, 0.43 mmol) were added, and the solution was heated to 70 ºC for 1 h. The solution was neutralized to pH 7 with saturated aqueous ammonium chloride (200 mL). The aqueous phase was extracted three times with ethyl acetate. The combined organics were washed with saturated aqueous sodium chloride, dried over anhydrous magnesium sulfate, filtered, and concentrated. The residue was purified by flash chromatography (silica gel, 0-25% ethyl acetate/hexane gradient) to afford the title compound (2.79 g, 75%). ^{1}H NMR (300 MHz, DMSO-d_6) δ 9.87 (s, 1H), 7.52 (d, J = 2.6 Hz, 1H), 7.41 – 7.30 (m, 2H), 7.24 (ddd, J = 8.8, 2.6, 0.3 Hz, 1H), 7.14 – 7.05 (m, 2H), 6.94 – 6.87 (m, 2H), 3.03 (d, J = 0.3 Hz, 3H). MS (ESI+) m/z 358.8 $(M+NH_4)^+$

4-(2-(2,4-Difluorophenoxy)-5-nitrophenyl)-6-methyl-1H-pyrrolo[2,3-c]pyridin-7(6H)-one (63a). Compound **21** (1.68 g, 3.81 mmol), 2,4-difluorophenol (0.44 mL, 4.6 mmol), and cesium carbonate (1.55 g, 4.76 mmol) were combined in DMSO (40 mL) and heated at 110 °C for 45 min. The

mixture was cooled, diluted with 200 mL of ethyl acetate, washed successively with brine and saturated aqueous sodium bicarbonate, and then dried over anhydrous magnesium sulfate. After filtration and solvent removal, the residue was purified by flash chromatography (silica gel, 0-100% ethyl acetate/heptane) to provide the title compound (0.986 g, 65%). ^{1}H NMR (300 MHz, DMSO-d_6) δ 12.10 (bs, 1H), 8.30 (d, J = 2.9 Hz, 1H), 8.19 (dd, J = 9.1, 2.9 Hz, 1H), 7.58 – 7.40 (m, 3H), 7.29 (t, J = 2.7 Hz, 1H), 7.23 – 7.12 (m, 1H), 6.95 (dd, J = 9.1, 1.1 Hz, 1H), 6.29 (dd, J = 2.8, 1.7 Hz, 1H), 3.57 (s, 3H). MS (ESI+) m/z 398.2 $(M+H)^+$.

4-(5-Amino-2-(2,4-difluorophenoxy)phenyl)-6-methyl-1H-pyrrolo[2,3-c]pyridin-7(6H)-one (63b). Compound **63a** (0.360 g, 0.906 mmol), iron powder (0.253 g, 4.53 mmol), and ammonium chloride (0.097 g, 1.8 mmol) were combined in ethanol (10 mL), THF (10 mL), and water (3 mL), and the mixture was heated under reflux for 2 h. The reaction mixture was cooled to just below reflux and vacuum filtered through Celite, and the filter cake washed with warm MeOH (3 x 50 mL). The eluent was concentrated under reduced pressure. The resulting residue was neutralized with saturated aqueous sodium bicarbonate, and the aqueous layer extracted with ethyl acetate (3 x 100 mL). The combined organics were washed with brine, dried over anhydrous magnesium sulfate, gravity filtered, and concentrated to provide the title compound (0.33 g, quant.). ^{1}H NMR (400 MHz, DMSO-d_6) δ 11.95 (bs, 1H), 7.28-7.18 (m, 2H), 7.18 (s, 1H), 6.84 (m, 1H), 6.82-6.73 (m, 2H), 6.73 (d, J = 2.8 Hz, 1H), 6.58 (dd, J = 8.6, 2.8 Hz, 1H), 6.22 (m, 1H), 5.09 (bs, 2H), 3.50 (s, 3H). MS (ESI+) m/z 368.2 $(M+H)^+$.

N-(4-(2,4-Difluorophenoxy)-3-(6-methyl-7-oxo-6,7-dihydro-1H-pyrrolo[2,3-c]pyridin-4-yl)phenyl)ethanesulfonamide (63). Compound **63b** (333 mg, 0.906 mmol) and triethylamine (0.379 mL, 2.72 mmol) were combined in dichloromethane (40 mL). Ethanesulfonyl chloride (466 mg, 3.63 mmol) was added dropwise and the solution was stirred at ambient temperature for 1 h. The reaction mixture was concentrated under reduced pressure, 1,4-dioxane (20 mL) and 10% aqueous sodium hydroxide (5 mL) were added, and the solution heated at 70ºC for 1 h. The solution was neutralized

with saturated ammonium chloride (100 mL) to pH 8 and the aqueous phase extracted with ethyl acetate (3 x 75 mL). The combined organic layers were washed with brine, dried over anhydrous magnesium sulfate, filtered, and concentrated. The residue was purified by reverse phase chromatography (C18, 0-100% acetonitrile/water, 0.1% TFA), to provide the title compound (0.306 g, 74%). ^{1}H NMR (300 MHz, DMSO) δ 12.04 (bs, 1H), 9.77 (s, 1H), 7.42-7.31 (m, 2H), 7.32-7.25 (m, 2H), 7.19 (dd, *J* = 8.8, 2.7 Hz, 1H), 7.13-6.93 (m, 2H), 6.91 (d, *J* = 8.7 Hz, 1H), 6.27-6.22 (m, 1H), 3.53 (s, 3H), 3.11 (q, *J* = 7.3 Hz, 2H), 1.23 (t, *J* = 7.3 Hz, 3H). MS (ESI+) m/z 460.1 $(M+H)^{+}$. ^{13}C NMR (101 MHz, DMSO) δ 157.5 (dd, *J* = 242.6, 10.8), 153.9, 152.7 (dd, *J* = 248.9, 12.9), 150.1, 139.8 (dd, *J* = 11.3, 3.4), 134.0, 129.3, 129.2, 127.9, 126.8, 123.2, 122.9, 121.5 (dd, *J* = 9.9, 1.5), 118.1, 111.7 (dd, *J* = 22.8, 3.4), 109.9, 105.4 (dd, *J* = 27.5, 22.4), 102.4, 45.1, 35.5, 8.0.

▪ ANCILLARY INFORMATION

Supporting Information

Additional information for the TR-FRET BRD4 binding assay, the MX-1 proliferation assay, and the BRD4 engagement luciferase reporter assay, including representative curves for compound **63**, are provided. Descriptions of the metabolic pathways analysis experiments, the murine multiple myeloma xenograft model, the plasma protein binding assay, isothermal titration calorimetry studies, bromodomain selectivity screening, and CEREP panel screening, as well as chemistry schemes and experimental procedures for compounds **38-62** and **64-120** are also provided (Schemes S1-S7 and Table S3). Molecular formula strings (CSV) are provided.

Accession Codes

Atomic coordinates of BRD4 BDII bound to compounds **11** (PDB code SUVZ), **19** (PDB code SUVY), and **24** (PDB code SUVX) have been deposited with the Protein Data Bank. Authors will release the atomic coordinates and experimental data upon article publication.

AUTHOR INFORMATION

Corresponding Author

***E-mail:** keith.f.mcdaniel@abbvie.com. Phone: 1-847-935-8318

ACKNOWLEDGEMENTS AND DISCLOSURES

This research used resources at the Industrial Macromolecular Crystallography Association Collaborative Access Team (IMCA-CAT) beamline 17-ID, supported by the companies of the Industrial Macromolecular Crystallography Association through a contract with Hauptman-Woodward Medical Research Institute.

This research used resources of the Advanced Photon Source, a U.S. Department of Energy (DOE) Office of Science User Facility operated for the DOE Office of Science by Argonne National Laboratory under Contract No. DE-AC02-06CH11357.

All authors are current or former AbbVie employees. The design, study conduct, and financial support for this research were provided by AbbVie. AbbVie participated in the interpretation of data, review, and approval of the publication.

ABBREVIATIONS USED

BD, bromodomain; BET, bromodomain and extra-terminal; TGI, tumor growth inhibition; TR-FRET, time-resolved fluorescence energy transfer.

REFERENCES

1. Arney, K. L. and Fisher, A.G. Epigenetic aspects of differentiation. *J. Cell Sci.* **2004,** *117*, 4355-4363.
2. Muller, S., Filippakopoulos, P. and Knapp, S. Bromodomains as therapeutic targets. *Expert Rev. Mol. Med.* **2011**, *13*, e29.

3. Wang, C-Y. and Filippakopoulos, P. Beating the odds – BETs in disease. *Trends in Biochem. Sci.* **2015**, *40*, 468-479.

4. For a recent comprehensive perspectives article on bromodomain inhibitors, see Romero, F. A.; Taylor, A. M.; Crawford, T. D.; Tsui, V.; Cote, A.; Magnuson, S. Disrupting acetyl-lysine recognition: Progress in the development of bromodomain inhibitors. *J. Med. Chem*. **2016**, *59*, 1271-1298.

5. Filappakopoulos, P., Picaud, S., Mangos, M., Keates, T., Lambert, J-P., Barsyte-Lovejoy, D., Felletar, I., Volkmer, R., Muller, S., Pawson, T., Gingras, A-C., Arrowsmith, C. H., and Knapp, S. Histone recognition and large-scale structural analysis of the human bromodomain family. *Cell* **2012**, *149*, 214-231.

6. Mitsubishi Tanabe Pharma Corporation. Antitumor agent. WO2009084693. **2009**.

7. Filippakopoulos, P.; Qi, J.; Picaud, S.; Shen, Y.; Smith, W. B.; Fedorov, O.; Morse, E. M.; Keates, T.; Hickman, T. T.; Felletar, I.; Philpott, M.; Munro, S.; McKeown, M. R.; Wang, Y.; Christie, A. L.; West, N.; Cameron, M. J.; Schwartz, B.; Heightman, T. D.; La Thangue, N.; French, C. A.; Wiest, O.; Kung, A. L.; Knapp, S.; Bradner, J. E. Selective inhibition of BET bromodomains. *Nature* **2010**, *468*, 1067−1073.

8. Noel, J. K; Iwata, K.; Ooike, S.; Sugahara, K.; Nakamura, H.; Daibata, M. Development of the BET bromodomain inhibitor OTX015. *Mol. Cancer Ther.* **2013**, *12(11 Suppl)*, C244.

9. Nicodeme, E.; Jeffrey, K. L.; Schaefer, U.; Beinke, S.; Dewell, S.; Chung, C.-W.; Chandwani, R.; Marazzi, I.; Wilson, P.; Coste, H.; White, J.; Kirilovsky, J.; Rice, C. M.; Lora, J. M.; Prinjha, R. K.; Lee, K.; Tarakhovsky, A. Suppression of inflammation by a synthetic histone mimic. *Nature* **2010**, *468*, 1119−1123.

10. Dawson, M. A.; Prinjha, R. K.; Dittmann, A.; Giotopoulos, G.; Bantscheff, M.; Chan, W. I.; Robson, S. C.; Chung, C. W.; Hopf, C.; Savitski, M. M.; Huthmacher, C.; Gudgin, E.; Lugo, D.; Beinke, S.; Chapman, T. D.; Roberts, E. J.; Soden, P. E.; Auger, K. R.; Mirguet, O.; Doehner,

K.; Delwel, R.; Burnett, A. K.; Jeffrey, P.; Drewes, G.; Lee, K.; Huntly, B. J.; Kouzarides, T. Inhibition of BET recruitment to chromatin as an effective treatment for MLL-fusion leukaemia. *Nature* **2011**, *478*, 529−533.

11. Albrecht, B. K.; Gehling, V. S.; Hewitt, M. C.; Vaswani, R. G.; Cote, A.; Leblanc, Y.; Nasveschuk, C. G.; Bellon, S.; Bergeron, L.; Campbell, R.; Cantone, N.; Cooper, M. R.; Cummings, R. T.; Jayaram, H.; Joshi, S.; Mertz, J. A.; Neiss, A.; Normant, E.; O'Meara, M.; Pardo, E.; Poy, F.; Sandy, P.; Supko, J.; Sims, R. J.; Harmange, J.-C.; Taylor, A. M.; Audia, J. E. Identification of a benzoisoxazoloazepine inhibitor (CPI-0610) of the bromodomain and extra-terminal (BET) family as a candidate for human clinical trials. *J. Med. Chem.* **2016**, *59*, 1330-1339.
12. Gosmini, R.; Nguyen, V. L.; Toum, J.; Simon, C.; Brusq, J.-M. G.; Krysa, G.; Mirguet, O.; Riou-Eymard, A. M.; Boursier, E. V.; Trottet, L.; Bamborough, P.; Clark, H.; Chung, C.-W.; Cutler, L.; Demont, E. H.; Kaur, R.; Lewis, A. J.; Schilling, M. B.; Soden, P. E.; Taylor, S.; Walker, A. L.; Walker, M. D.; Prinjha, R. K.; Nicodeme, E. The Discovery of I-BET726 (GSK1324726A), a potent tetrahydroquinoline ApoA1 up-regulator and selective BET bromodomain inhibitor. *J. Med. Chem.* **2014**, *57*, 8111-8131.
13. (a) Filippakopoulos, P.; Knapp, S. The bromodomain interaction module. *FEBS Lett*. **2012**, *586*, 2692-2704. (b) Filippakopoulos, P.; Picaud, S.; Mangos, M.; Keates, T.; Lambert, J-P.; Barsyte-Lovejoy, D.; Felletar, I.; Volkmer, R.; Müller, S.; Pawson, T.; Gingras, A-C.; Arrowsmith, C. H.; Knapp, S. Histone recognition and large-scale analysis of the human bromodomain family. *Cell* **2012**, *149*, 214-231.
14. For recent reviews on the clinical development of BET bromodomain inhibitors, see (a) Theodoulou, N. H.; Tomkinson, N. C. O.; Prinjha, R. K.; Humphreys, P. G. Clinical progress and pharmacology of small molecule bromodomain inhibitors. *Curr. Opin. Chem. Biol*. **2016**, *33*, 58-66. (b) Liu, Z.; Wang, P.; Chen, H.; Wold, E. A.; Tian, B.; Brasier, A. R.; Zhou, J. Drug

discovery targeting bromodomain-containing protein 4 (BRD4) *J. Med. Chem.* **2017**, *60*, 4533-4558.

15. Wang, L.; Pratt, J. K.; Soltwedel, T.; Sheppard, G. S.; Fidanze, S.; Liu, D.; Hasvold, L. A.; Mantei, R. A.; Holms, J.; McClellan, W.; Wendt, M.; Wada, C.; Frey, R.; Hansen, T. M.; Hubbard, R.; Park, C.; Li, L.; Magoc, T.; Albert, D. H.; Lin, X.; Warder, S.; Kovar, P.; Huang, X.; Wilcox, D.; Wang, R.; Rajaraman, G.; Petros, A.; Hutchins, C.; Torrent, M.; Panchal, S.; Sun, C.; Elmore, S. W.; Rosenberg, S.; Shen, Y.; McDaniel, K. F.; Kati, W. Fragment-based, structure-enabled discovery of novel pyridone and pyridone macrocycles as potent BET family bromodomain inhibitors. *J. Med Chem*. **2017**, *60*, 3828-3850.
16. (a) ClinicalTrial.gov identifier: NTC02391480. (b) Wang, L.; Pratt, J. K.; McDaniel, K. F.; Dai, Y.; Fidanze, S. D.; Hasvold, L. A.; Holms, J. H.; Kati, W. M.; Liu, D.; Mantei, R. A.; McClellan, W. J.; Sheppard, G. S.; Wada, C. K. Bromodomain inhibitors. WO2013097601, December 11, 2012.
17. Miyaura, N.; Suzuki, A. Palladium-catalyzed cross-coupling reactions of organoboron compounds. *Chem. Rev*. **1995**, *95(7)*, 2457-2483.
18. Smith, J. A.; White, E. A.; Sowa, M. E.; Powell, M. L.; Ottinger, M.; Harper, J. W.; Howley, P. M. Genome-wide SiRNA screen identifies SMCX, EP300, and Brd4 as E2-dependent regulators of human papillomavirus oncogene expression. *Proc. Natl. Acad. Sci. U. S. A.* **2010**, *107*, 3752-3757.
19. Shi, J.; Vakoc, C. R. The mechanisms behind the therapeutic activity of BET bromodomain inhibition. *Mol. Cell* **2014,** *54*, 728-736.
20. LipE values were calculated according to the following equation: LipE = p*Ki* – cLogP. See Leeson, P. D.; Springthorpe, B. The Influence of drug-like concepts on decision-making in medicinal chemistry. *Nat. Rev. Drug Discovery* **2007**, *6*, 881-890.

21. Bayden, A. S.; Moustakas, D. T.; Joseph-McCarthy, D.; Lamb, M. L. Evaluating free energies of binding and conservation of crystallographic waters using SZMAP. *J. Chem. Inf. Model.* **2015**, *55*, 1552-1565. OpenEye Scientific Software, Santa Fe, NM.

22. Researchers at Genentech and Constellation recently published their work on the identification of pyrrolopyridone as a useful core for generation of inhibitors that generate inducible binding conformations for BRD4, TAF1(2), BRD9, and CECR2 bromodomains: Crawford, T. D.; Tsui, V.; Flynn, E. M.; Wang, S.; Taylor, A. M.; Cote, A.; Audia, J. E.; Beresini, M. H.; Burdick, D. J.; Cummings, R.; Dakin, L. A.; Duplessis, M.; Good, A. C.; Hewitt, M. C.; Huang, H-R.; Jayaram, H.; Kiefer, J. R.; Jiang, Y.; Murray, J.; Nasveschuk, C. G.; Pardo, E.; Poy, F.; Romero, F. A.; Tang, Y.; Wang, J.; Xu, Z.; Zawadzke, L. E.; Zhu, X.; Albrecht, B. K.; Magnuson, S. R.; Bellon, S.; Cochran, A. G. Diving into the water: Inducible binding conformations for BRD4, TAF1(2), BRD9, and CECR2 bromodomains. *J. Med. Chem.* **2016**, *59*, 5391-5402.

23. Dhalluin, C.; Carlson, J. E.; Zeng, L.; He, C.; Aggarwal, A. K.; Zhou, M-M. Structure and ligand of a histone acetyltransferase bromodomain. *Nature* **1999**, *399*, 491-496.

24. Hasvold, L. H.; Sheppard, G. S.; Wang, L.; Fidanze, S. D.; Liu, D.; Pratt, J. K.; Mantei, R. A.; Wada, C. K.; Hubbard, R.; Shen, Y.; Lin, X.; Huang, X.; Warder, S. E.; Wilcox, D.; Li, L.; Buchanan, F. G.; Smithee, L.; Albert, D. A.; Magoc, T. J.; Park, C. H.; Petros, A. M.; Panchal, S. C.; Sun, C.; Kovar, P.; Soni, N. B.; Elmore, S. W.; Kati, W. M.; McDaniel, K. F. Methylpyrrole inhibitors of BET bromodomains. *Bioorg. Med. Chem. Lett.* **2017**, *27*, 2225-2233.

25. Lipinski, C. A.; Lombardo, F.; Dominy, B. W.; Feeney, P. J. Experimental and computational approaches to estimate solubility and permeability in drug discovery and development settings. *Adv. Drug Del. Rev.* **1997**, *23*, 3-25.

26. Bui, M. H.; Lin, X.; Albert, D. H.; Li, L.; Lam, L. T.; Faivre, E. J.; Warder, S.; Huang, X.; Wilcox, D.; Donawho, C. K.; Sheppard, G. S.; Wang, L.; Fidanze, S.; Pratt, J. K.; Liu, D.; Hasvold, L.; Uziel, T.; Lu, X.; Kohlhapp, F.; Fang, G.; Elmore, S. W.; Rosenberg, S. H.;

McDaniel, K. F.; Kati, W. M.; Shen, Y. Comprehensive in vitro and in vivo characterization of a novel BET family bromodomain inhibitor, ABBV-075, reveals sensitive cancer indications and combination strategies for BET inhibitors. *Cancer Res.* **2017**, *77*, 2976-2989.

27. Ghurye, R. R.; Stewart, H. J.; Chevassut, T. J. Bromodomain inhibition by JQ1 suppresses lipopolysaccharide-stimulated interleukin-6 secretion in multiple myeloma cells. *Cytokine* **2015**, *71(2)*, 415-7.

28. (a) Faivre, E. J.; Wilcox, D.; Lin, X.; Hessler, P.; Torrent, M.; He, W.; Uziel, T.; Albert, D. H.; McDaniel, K.; Kati, W.; Shen, Y. Exploitation of castration-resistant prostate cancer transcription factor dependencies by the novel BET inhibitor ABBV-075. *Mol. Cancer Res.* **2017**, *15(1)*, 35-44. (b) Lam, L. T.; Lin, X.; Faivre, E. J.; Yang, Z.; Huang, X.; Wilcox, D. M.; Bellin, R. J.; Jin, S.; Tahir, S. K.; Mitten, M.; Magoc, T. Bhathena, A.; Kati, W. M.; Albert, D. H.; Shen, Y.; Uziel, T. Vulnerability of small cell lung cancer to apoptosis induced by the combination of BET bromodomain proteins and BCL2 inhibitors. *Mol. Cancer Ther.* **2017**, *16 (8), 1511-1520*. (c) Lin, X.; Huang, X.; Uziel, T.; Hessler, P.; Albert, D. H.; Roberts-Rapp, L. A.; McDaniel, K. F.; Kati, W. K.; Shen, Y. HEXIM-1 as a robust pharmacodynamic marker for monitoring target engagement of BET family bromodomain inhibitors in tumors and surrogate tissues. *Mol. Cancer Ther.* **2017**, *16(2)*, 388-396.

Table of Contents Graphic

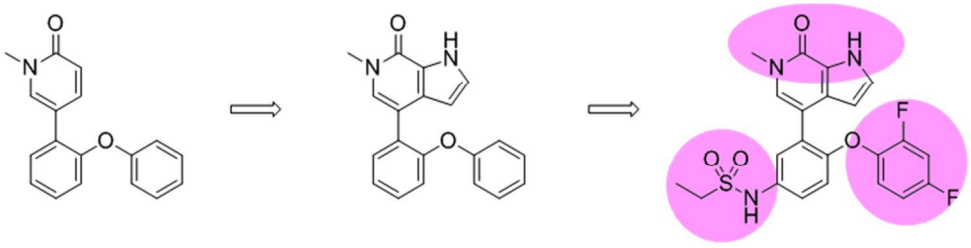

9

BRD4 TR-FRET K_i = 890 nM
BRD4 Engagement EC_{50} = 4100 nM
LipE = 1.8

19

BRD4 TR-FRET K_i = 48 nM
BRD4 Engagement EC_{50} = 550 nM
Limited metabolic stability
LipE = 2.8

63

BRD4 TR-FRET K_i = 1.5 nM
BRD4 Engagement EC_{50} = 20 nM
Human Liver Microsome $Cl_{int\ u}$ = < 3 L/hr/kg
LipE = 4.9